EFFECT OF EXCHANGE AND ABSORPTION POTENTIAL IN THE DISTORTED WAVE CALCULATION OF ELECTRON IMPACT EXCITATION OF AUTO IONIZING STATE OF RUBIDIUM

VINCENT ONYANGO OTHIENO NUNDA AGUTU

I56/CE/23526/2011

A THESIS SUBMITTED IN PARTIAL FULFILLMENT OF THE REQUIREMENTS FOR THE AWARD OF THE DEGREE OF MASTER OF SCIENCE IN THE SCHOOL OF PURE AND APPLIED SCIENCES OF KENYATTA UNIVERSITY.

NOVEMBER 2016

DECLARATION

This is my original work and has not been presented for a degree in any other university or any other award in any University.

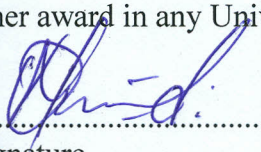

Signature

Date

Vincent Onyango Othieno Nunda Agutu

Department of Physics

Kenyatta University

We confirm that the candidate under our supervision carried out the work reported in this thesis.

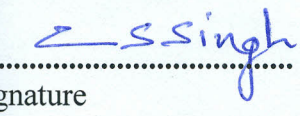

Signature

Date

Dr. C.S. Singh

Department of Physics

Kenyatta University

Signature

Date

Prof. John Okumu

Department of Physics

Kenyatta University

DEDICATION

This thesis is dedicated to my wife Purity, my God given son Mike and my supervisor C.S Singh.

ACKNOWLEDGEMENT

May I start by thanking my supervisors Dr C.S.Singh and Prof J. Okumu whose extensive support in terms of moral advice, encouragement and material works have assisted me in the research. And especially for the tireless guidance and patience of Dr C.S.Singh during this research work.

To physics department laboratory staff I wish to acknowledge and appreciate them for their support.

To my friends Aguyo Apolo and the late Daniel Porgon fruitful for their support and encouragement.

I am also greatful to Purity my wife, my mother Florence Agutu and my son Mike for their patience and encouragement during my studies.

Above all, thanks to God who gave me the strength, wisdom and good health to study and attain his will.

TABLE OF CONTENTS

LIST OF TABLES

LIST OF FIGURES

ABBREVIATIONS AND ACRONYMS

CCC - Convergent Close Coupling

CPB - Coulomb Projected Born

DCS - Differential Cross Section

DWBA1 - First order Distorted Wave Born Approximation

DWM - Distorted Wave method

FBA - First Born Approximation

ICS - Integral Cross Sections

MFBA - Modified First Born Approximation

MZ - Multi Zeta wave functions

Rb - Rubidium

RDW - Relativistic Distorted Wave method

ABSTRACT

Study of electron impact excitation of autoionizing states of alkali atoms is very important because it can explain the additional peaks which appear in the ionization curve of the alkali atoms. Very many researches have been made on the research of electron impact excitation of autoionizing states of alkalis using close coupling method, R-matrix and Distorted Wave Method. But in the Distorted Wave applied to electron impact excitation of rubidium atom only the real potential i.e. static or static and exchange potential has been used. That is why in this study complex distortion potential which includes static, exchange and absorption potential, has been used for electron impact excitation of lowest autoionizing state of rubidium atom using a distorted wave method. Initial and final state wave function of the projectile electron is distorted by the complex potential. Differential and integral cross section and angular correlation parameter have been calculated and compared with the available theoretical and experimental results. Numerical calculations have been done using a modified dwba1 fortran computer program which was originally made for hydrogen atom. From the comparison of the results, it is observed that in general the electron impact excitation cross section results are higher around excitation threshold energy. This can be attributed to the exchange process which takes place in the case of electron impact and also due to larger interaction between the projectile and the target. It is also observed that the absorption potential lowers the cross section and brings it closer to the experimental results. Alignment parameter results indicate that the integral cross section results for m=0 level are larger compared to m=1 level for impact energies up to about 400eV beyond which integral cross-sections for the magnetic sublevel m=1 become greater. The lambda parameter indicates that more particles are scattered towards m=0 for electron impact.

CHAPTER 1

INTRODUCTION

1.1 Background of the study

The study of atomic collision physics plays an important role in the development of different areas of physics mainly astrophysical science, laser physics, light industry, medicine and material science. For this reason, scientists have developed experimental and theoretical tools to help understand the field of atomic collisions in-depth in the form of evalution of differential, integral cross sections and angular correlation parameters.Research on electron atomic collision has seen rapid increase in interests, using theoretical and experimental approaches. This is due to the fact that these processes produce a clear means of investigating the dynamics of the collision process. However, it is mostly because the information is relevant in many areas.

The study of atomic collision involves the scattering of a projectile by a target. A projectile may be any charged particle e.g. electron, positron, proton, an ion and any atom or ion or a molecule may be the target. Experimentally, a beam of free particles is scattered from the target and the scattered particles detected in the asymptotic region (Joachain,1975). A theoretical study can be done using semi classical methods or quantal approaches. Semi classical methods include semi classical impact parameter method, classical trajectory andmontecarlo method, classical impulse and binary encounter approximation, eikonal approximation, multi- channel elkonal treatment and Glauber approximation. Quantal approaches are classified into perturbative and non perturbativemethods.Perturbative methods include Born series,

Eikonal series, distorted wave series(Joachain, 1975) and many body theory(Madison and Bartschat, 1996. Non perturbativemethod includes R-matrix(Burke and Berrington, 1993), convergent close coupling(McCarthy and Weigold, 1995) andvariational methods.

Distorted wave approximation methods were introduced because the Born approximation failed to give accurate account of differential cross-sections for low impact energies and large scattering angles. In distorted wave approximation, the incident electron is taken to be elastically scattered by the initial state atomic potential. In the direct process, the incident electron makes a transition to state in which it is being elastically scattered by final-state atomic potential. If the excitation of the atom is through exchange process, the incident electron is captured into a bound state of the atom, while one of the initially bound electrons is ejected into an elastic-scattering state. The transition between the initial and final elastic state is calculated by perturbation method.

In experimental approach, developments have taken a great stride and this has also contributed greatly in the atomic collision and its applications. Instruments used have also been refined to give accurate result but the basic concept still remains the sameA typical set-up for electron-atom scattering experiments is illustrated in figure 1.1 (McCarthy and Weigold, 1995).

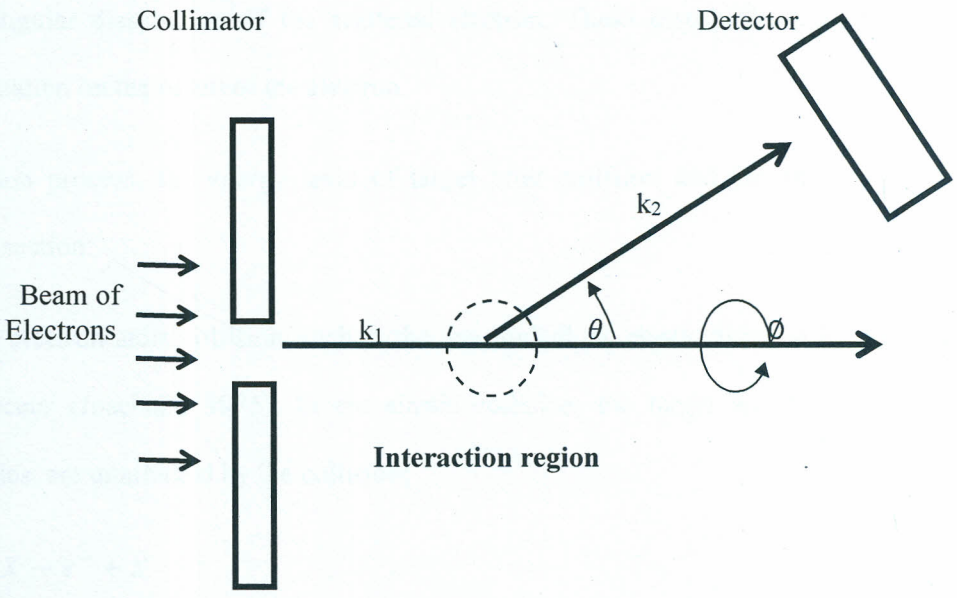

Figure 1.1 Schematic diagram of a scattering experiment

The electron gun produces electrons and accelerates them at the required velocity towards the target atom for example rubidium. The incident electron is monoenergetic with a momentum of k_1. When a collision takes place, an electron with a momentum $k_2$is deflected from its path and the target atom is either excited or ionized or remains in the same state. The deflected electron is detected by the detector. The direction of the scattered electron is determined by the polar $\theta$and azimuthal angles$\emptyset$.

The experiment (theory) measure (calculate) the differential cross-sectionswhich are a measure of the probability that the electron will be scattered in a given direction, determined by the two angles θ and$\emptyset$. However, integral cross section can be determined using differential cross- section values by integrating them over angle θ and $\emptyset$. Differential cross-section measurements are carried out by crossing the target atom with monoenergetic electron beam usually at 90^0 and determining the energy

and angular distribution of the scattered electron. These distributions contain the information on the natureof the electron

collision process, the energy level of target after collision and the corresponding cross-section.

In the electron-atom collision, such as the one studied, an elastic or inelastic collision can occur (Joachain, 1975). In the elastic collision, the target and the projectile energies are unaffected by the collision;

$$e^- + X \rightarrow e^- + X \qquad (1.0)$$

where$X$ represent an atom

In an inelastic collision, there is some energy transfer between the incident electron and the target. This results in either the target electron moving to higher energy level (equation 1.1) or one or more electron being removed from the atom (equation 1.2);

$$e_i^- + X \rightarrow e_s^- + X^* \quad \text{(excitation)} \qquad (1.1)$$

or

$$e_i^- + X \rightarrow e_s^- + X^+ + e_e^- \quad \text{(ionization)} \qquad (1.2)$$

where e_i^-, e_s^- ande_e^- are respectively the incident,scattered and ejected electrons. $X^*$is the excited state of$X$.

The ionization can take place in two ways, either by direct process or through the excitation of the autoionizing state and then its subsequent decay to its ion by ejecting an electron. It can be shown as follows;

$$e_i^- + X \xrightarrow{direct} e_s^- + e_e^- + X^+ \qquad (1.3)$$
$$\searrow \quad \nearrow$$
$$e_i^- + X^*$$

Autoionization

Here X^* is an autoionizing state. These autoionizing states lie above the first ionization threshold of the atom.

In inelastic scattering comparison of measured and calculated cross sections is important in the understanding of the nature of interactions of electrons with atoms. Cross sections for electron-atom scattering are important in laser development and inplasma physics (McCarthy and Weigold, 1995).

Elastic scattering cross sections are useful in X-ray photoelectron spectroscopy, XPS, and Auger-electron spectroscopy, AES, (Jablonski*et al.*, 2004) where the signal electrons are elastically scattered from within metal surfaces. These cross sections also provide vital input in the Monte- Carlo simulation of conduction of electrons in solids (Jablonski*et al.*, 2004)

1.2 Statement of research problem

In this study the effect of exchange and absorption potential has been investigated using distorted wave calculation method of electron impact excitation of lowestautoionizing state of rubidium by calculating the differential and integral cross sections.Integral cross sections are compared in the energy range of 15.3eV to 1000eV using multi zeta wave functions. The results for ICS have been compared to those of Pangantiwar and Srivastava (1987) and Borovik*et al.* (2012, 2013).An exact agreement among these theoretical approaches and between theory and experiment is

generally lacking which makes further work on the problem necessary. Angular correlation parameters and alignment parameter for the excited state have also been calculated and compared with Pangantiwar and Srivastava (1987) results.

1.3 Objectives of the study

1.3.1 General objective

The general objective of this research was to study the effect of exchange and absorption potential in the distorted wave calculation of electron impact excitation of lowest autoionizing state of rubidium.

1.3.2 Specific objectives

The specific objectives were as follows;

i. To formulate the T-matrix for the electron impact excitation of autoionizing state of rubidium in distorted wave method.

ii. To modify the DWBA 1 program for electron impact excitation of rubidium atom.

iii. To determine the differential and integral cross section for electron impact excitation of autoionizing state of rubidium using static potential as the distortion potential.

iv. To determine the differential and integral cross section for electron impact excitation of autoionizing state of rubidium using static plus exchange potential as the distortion potential.

v. To determine the differential and integral cross section for electron impact excitation of autoionizing state of rubidium using static plus exchange and absorption potential as the distortion potential

vi. To determine angular correlation parameters.

vii. To compare the present result obtained in (iii), (iv) and (v) among themselves and with other available theoretical and experimental results to see the effect of exchange and absorption potential on differential and integral cross sections.

1.4 Rationale of the study

The study of atomic collision has grown enormously since the Rutherford scattering of ∝particles by atoms in 1911. Many methods have been used both in theoretical and experimental approaches (McConkey, 2005). The experimental and theoretical literature available are not in good agreement hence there is a need for this study.The data have been continuously assessed in order to provide the most reliable findings for application in various fields. Even though so many researches have been made onscattering leading to autoionization, not much have been done in the area of the effect of exchange and absorption potential in the distorted wave calculation of electron impact excitation of autoionizing state of rubidium. It would be interesting to see the data obtained using distorted wave method compared with Borovik*et al* (2012,2013) and Pangantiwar and Srivastava (1987) and get an idea of the effect of exchange and absorption potential on the cross sections and therefore in this pursuit this work was done.

Apart from their fundamental role as a test ground for various theoretical approaches, atomic collisions are of critical importance in many fields including the physics of stars, the upper atmosphere , lasers and plasmas.

CHAPTER 2

LITERATURE REVIEW

2.1 Electron impact excitation of autoionizingstate of rubidium

Borovik *et al.* (2013) studied electron impact excitation of autoionizing states of rubidium experimentallyand theoretically by performing fully relativistic B-spline R-matrix calculation. The data revealed a strong resonance excitation of all states. Good agreement between experiment and theory was found for the lowest $^2P_{3/2,1/2}$ states and, to some extent, also for the $^4P_{1/2}$ state, while significant deviations between experiment and theory remained for the $^4P_{3/2,5/2}$ states

Borovik*et al.* (2012)studiedtheautoionizationcrosssectionofrubidium atoms in the electron impact energy range from the lowest autoionization threshold up to 50 eV by measuring the total normalized intensities of ejected-electron spectra arising from the decay of the $4p^5n_1l_1n_2l_2$autoionizing levels. A strong negative-ion resonances was found to be present near the excitation thresholds of the lowest levels in $5s^2$ and 4d5s configurations and was concluded to be the reason for the quick rise of the autoionization cross section between 15.3 and 18.5 eV.

Ross and Ottley (1975) studied the ejection of electron of rubidium autoionizing levels obtained by electron impact excitation. Autoionizing transitions in rubidium were observed by measuring the energy spectrum of electrons ejected at 90^0 to the direction of an incident 500 eV electron beam.

Using first Born approximation (FBA), modified first Born approximation (MFBA) and Vainshtein approximation, Tiwary and Rai (1975) studied electron impact excitation of the lowest autoionizing levels of alkali metal atoms(K, Rb and Cs)where the total cross section were calculated. FBA results differ greatly from the results obtained by the application of the MFBA and the Vainshtein approximation. The inclusion of the acceleration effect not only lowers the cross section but also shifts the peak of the excitation cross section curve to lower incident energies. The excitation cross section obtained by the use of the Vainshtein approximation differ (are smaller) from the FBA results for small incident energies near the threshold. But at high energies the results of all the three approximations tend towards each other. The Vainshtein approximation leads to a smaller excitation cross section at all values of the incident energy and the cross section curve reaches its maximum more slowly.

Nygaard (1975) carried out an experimental study on electron impact autoionization in heavy alkali metals. Here, autoionizing levels in cesium, rubidium and potassium were studied by electron impact in a crossed beam apparatus.Rubidiumand potassium atom, showed agreement with the energies at which the autoionization peaks occur, but not with the absolute magnitudes predicted by Roy and Rai (1973). The resonance-type behavior was supported by his experimental data.

2.2 Electron impact excitation of autoionizing states of alkalis using distorted wave method

Pangantiwar and Srivastava (1987) studied electron impact excitation of autoionizing levels in alkalis using Distorted Wave Method approach for incident electron energy varying from the threshold energy of about 15.3 eV to 1000 eV. In this study, multi-

zeta RHF wave functions and the initial and final state static potentials as the distortion potentials for the initial and final distorted waves respectively were applied. For Rb, results for the polarization parameter, alignment parameter and the integral cross section (ICS) for electron impact excitation of the lowest autoionizing state were presented. Their results for ICS with exchangeand without exchange were almost the same at higher energies of about 500 eV up to 1000 eV.

Kaur and Srivastava (1999) carried out relativistic distorted-wave (RDW) calculations for the electron impact excitation of the lowest autoionizing states $np^5(n+1)s^2$, $^2P_{3/2,1/2}$ in Na(n = 2), K(n = 3), Rb(n = 4) and Cs(n = 5) alkali atoms from the ground $np^6(n+1)s$, $^2S_{1/2}$ state. Detailed results in the range of near threshold to 1.5 keV incident electron energies are obtained for total cross sections of the magnetic sub states of the individual $^2P_{3/2}$ and $^2P_{1/2}$ states. RDW calculation excluding the exchange effect and relativistic Born approximation calculation are also performed for comparison. The results are compared and discussed in the light of earlier available theatrical and experimental data.

The results for Na and Kcomparereasonablywellwithexperiments of Matterstock*et al.* (1995) and Feuerstein *et al.* (1998).

Oketch (2013) applied the distorted wave method to electron impact excitation of the lowest autoionizing state of rubidium. In his distorted wave method the projectile electron wave functions were distorted only by the static potentials of the target atom. Exchange and absorption potentials were not included. His result for integral cross section agreed well with experimental result for Borovik*et al.*(2012) at low energies.Distorted wave results without exchange is higher near threshold than distorted wave result with exchange process. Near threshold energies, the integral

cross sections are large and so the maximum contribution of autoionization would be at the threshold of excitation of the autoionizing level.

CHAPTER 3

THEORETIAL BACKGROUND OF APPROXIMATION METHODS

3.1 Introduction to theoretical framework

In this chapter, theoretical methods used in atomic collisions are discussed. Various theoretical methods have been used in the study of electron atom scattering. These methods can be classified into two categories; semi classical and quantum mechanical.

3.2 Quantum Mechanical Methods

3.2.1 The Born approximation

The Born approximation is widely used in scattering theory and it is essentially a perturbation type expansion of the wave function or the scattering amplitude in powers of the interaction potential. The scattering amplitude is written as

$$f = -\frac{1}{4\pi}\langle\psi_{kf}|U + UG_0^+U + UG_0^+UG_0^+U + \cdots|\psi_{ki}\rangle \tag{3.1}$$

whereΨ_{k_f} is the product of final plane wave $e^{ik_f.r}$ of the projectile and the final target wave function φ_f .$\Psi_{k_i}$is the product of the initial plane wave $e^{ik_i.r}$ of the incident particle and the initial atomic wave function φ_i .$U$is the interaction potential and the function G_0^+ is outgoing Green's function given as

$$G_0^+(k,r,r') = \frac{1}{4\pi}\frac{e^{ik|r-r'|}}{|r-r'|} \tag{3.2}$$

The first term in the equation3.1 is the first Born approximation to the scattering amplitude and is given by equation 3.3

$$f_{B1} = -\frac{1}{4\pi}\left\langle \psi_{k_f} \middle| U \middle| \psi_{k_i} \right\rangle \tag{3.3}$$

When the first two terms in the equation 3.1 are taken then it is the second Born approximation f_{B2} and so on. The first Born approximation is valid generally for high impact energies when the interaction is for a very short duration and the projectile waves (incident and scattered) can be approximated as plane waves (Joachain,1975).

3.2.2 The coulomb –projected Born approximation

The Coulomb-projected Born approximation (CPB) consists basically of modifying the usual Born approximation by taking an explicit account of the Coulomb interaction between the projectile and the nucleus. The final state plane wave in the Born approximation is replaced by a Coulomb wave function corresponding to the nuclear charge. Different ways of taking this Coulomb interaction into account has led to different CPB methods, for example CPB approximation by Geltman (1971), Generalized CPB approximation by Stauffer and Morgan (1975) and a variable charge CPB approximation by Schaub-Shaver and Staufffer (1980). The approximations are useful in describing collisions of electrons and ions with target atoms and ions to give results that are better than Born approximation results.

3.2.3 The R-Matrix method

In this method the configuration space for the (N+1) electron-atom system is divided into two regions depending on the relative distance, r , between the projectile electron and the atomic nucleus. One is the internal region (r<a) and the other is the external

region (r>a). In the internal region the interaction is strong and electron exchange is important while in the external region the electron exchange can be neglected and hence, the collision can be described by coupled differential rather than integro–differential equations which often have an analytic solution or at least a solution which can be readily obtained by numerical method (Scott,2004). In this method the target eigenstates and pseudo states are written as linear sums of Slater orbital and the incident electron wave function is expanded in terms of orthogonal orbital which satisfy logarithmic boundary condition on the surface of the sphere. The Hamiltonian is then diagonalized in an appropriately chosen basis in the internal region and the cross sections calculated by solving the asymptotic problem in the external region (Burke and Berrington,1993).

3.2.4 The optical potential method

The idea of this method is to analyze the elastic scattering of a particle from a complex target by replacing the complicated interactions between the projectile and the target particles by an optical potential in which the incident particles move. This optical potential is also called a pseudo-potential. Once the optical potential is determined, the original many body problemreduces to a one –body problem. However, this reduction is in general a difficult task and approximations are necessary. For cases involving fast collisions, a multiple scattering approach is often used since it is convenient (Joachain,1975).

3.2.5 Convergent close coupling method

Just like R- matrix and other methods based on close coupling,convergent close coupling (CCC) is only suitable for elastic and inelastic scattering at lower impact

energies of the projectile. The CCC method relies on the close coupling formalism for solving the coupled equations without approximations (Bray *et al*, 2009). The convergence is tested by including an ever increasing set of states in the close coupling formalism. The target states are obtained by diagonalising the target Hamiltonian in an orthogonal Laguerre basis which ensures that the completeness is approached as the basis size increases. The CCC treats both the discrete and continuum parts of the target space through the close coupling formalism, this allows the validity of the CCC method to be independent of the projectile energy or the transition of interest (Fursa and Bray,1995).

3.2.6 The distorted wave methods

Distorted wave methods (DWM) were introduced because the Born approximation failed to give accurate accounts of differential cross-sections for low impact energies and large scattering angles. In the distorted wave approximation, the incident electron is taken to be elastically scattered by the initial state atomic potential. If the excitation of the atom is through direct process,the incident electron makes a transition to a state in which it is being elastically scattered by final-state atomic potential(Pangantiwar and Srivastava, 1987), if the excitation of the atom is through exchange process, the incident electron is captured into a bound state of the atom, while one of the initially bound electrons is ejected into an elastic-scattering state. In this case, the transition between the initial and final elastic state is calculated by perturbation method. This method is suitable for calculation of differential cross-section for electron impact excitation of atoms at intermediate and high incident energies.

DWM have been one of the most successful perturbative methods used especially at intermediate and high impact energies of projectiles. Their advantage lies in the leading term of the perturbation series expansion such that the distorted wave series converges faster than the Born series. Distorted wave method can also be applied to study electron molecule collision, electron impact ionization of atoms and collision processes among heavy particles. Distorted wave methods have been applied in various collision processes since it is quite successful in explaining various features of an excitation process for instance the effect of a particular distortion potential (Katiyar*et al.*, 1989). However, their limitation is that they give poor results at low incident energies. Distorted wave methods are more conveniently discussed within the framework of the two potential formatismdiscussed in section 3.3

3.3 Distorted wave formula using two potential scattering model

In this section the general formulation of the distorted wave approximation is described before specializing it to the particular case of electron rubidium scattering which will be discussed in chapter 4. The distorted wave methods are discussed within the framework of a two potential formalism where the interaction potential (V) is broken in a physically meaningful way into two parts one of which is treated exactly (U) and the other which is handled in an approximation way (W) (Joachain, 1975). That is in this model the interactions potential is divided into two parts i.e;

$$V = U + W \tag{3.4}$$

and the total Harmiltonian$H$ for the system is given as;

$$H = H_0 + V = H_0 + U + W \tag{3.5}$$

It is assumed that the equation;

$$(H_0 + U)\chi^{\pm} = E\chi^{\pm} \tag{3.6}$$

can be solved exactly. Here H_0 is the unperturbed part of the Harmiltonian and is given as;

$$H_0 = h_a + T \tag{3.7}$$

where$T$is the kinetic energy operator, $h_a$is the Hamiltonian of the target atom.$\chi$is the product of target wave function and the projectile wave function within the interaction region (distorted wave) and + (-) represents the outgoing (incoming) wave boundary conditions.

The transition matrix element for the scattering problem is expressed as;

$$T_{if} = \langle \varphi_f | V_f | \Psi_i^+ \rangle \tag{3.8}$$

Where φ_f is the product of the final target state wave function and the final plane wave function of the projectile in the asymptotic region and Ψ_i^+ is the total wave function of the system.

Making use of equation 3.4,equation 3.8 can be written as;

$$T_{if} = \langle \varphi_f | U_f + W_f | \Psi_i^+ \rangle \tag{3.9}$$

The total wave function with the incoming boundary conditions can be expressed as;

$$|\chi_f^-\rangle = |\varphi_f\rangle + \frac{1}{E_f - H_f - i\varepsilon} U_f |\varphi_f\rangle \tag{3.10}$$

Where $H_f = H_0 + U_f$ and this Hamiltonian satisfy equation (3.6). Equation (3.10) can also be written as;

$$\langle\varphi_f| = \langle\varphi_f| - \langle\varphi_f|U_f \frac{1}{E_f - H_f + i\varepsilon} \tag{3.11}$$

Expanding equation (3.9) and making use of equation (3.11), the transition matrix element can be written as;

$$T_{if} = \langle\varphi_f|U_f|\Psi_i^+\rangle + \langle\chi_f^-|W_f|\Psi_i^+\rangle - \left\langle\varphi_f\middle|U_f \frac{1}{E_f - H_f + i\varepsilon} W_f\middle|\Psi_i^+\right\rangle \tag{3.12}$$

The third term on the right hand side of equation 3.12 can be transformed by making use of the relation;

$$|\Psi_i^+\rangle = |\varphi_i\rangle + \frac{1}{E_f - H_f + i\varepsilon} V_i|\varphi_i\rangle \tag{3.13}$$

As (on the energy shell $E = E_i = E_f$);

$$\left\langle\varphi_f\middle|U_f \frac{1}{E_f - H_f + i\varepsilon} W_f\middle|\Psi_i^+\right\rangle = \left\langle\varphi_f\middle|U_f \frac{1}{E - H_f + i\varepsilon} W_f\middle|\varphi_i\right\rangle +$$

$$\left\langle\varphi_f\middle|U_f \frac{1}{E - H_f + i\varepsilon} W_f \frac{1}{E - H + i\varepsilon} V_i\middle|\varphi_i\right\rangle \tag{3.14}$$

And further making use of equation (3.11) we can write equation (3.14) as;

$$\left\langle\varphi_f\middle|U_f \frac{1}{E_f - H_f + i\varepsilon} W_f\middle|\Psi_i^+\right\rangle = \langle\chi_f^-|W_f|\varphi_i\rangle - \langle\varphi_f|W_f|\varphi_i\rangle +$$

$$\left\langle\varphi_f\middle|U_f \frac{1}{E - H_f + i\varepsilon} W_f \frac{1}{E - H + i\varepsilon} V_i\middle|\varphi_i\right\rangle$$

(3.15)

The operator identity;

$$\frac{1}{B}(B - A)\frac{1}{A} = \frac{1}{A} - \frac{1}{B}$$

is used with $A = E - H + i\varepsilon, B = E - H_f + i\varepsilon$ and recalling that

$H - H_f = W_f$, we find that;

$$\left\langle \varphi_f \middle| U_f \frac{1}{E-H_f+i\varepsilon} W_f \frac{1}{E-H+i\varepsilon} V_i \middle| \varphi_i \right\rangle = \left\langle \varphi_f \middle| U_f \frac{1}{E-H+i\varepsilon} V_i \middle| \varphi_i \right\rangle -$$

$$\left\langle \varphi_f \middle| U_f \frac{1}{E-H_f+i\varepsilon} V_i \middle| \varphi_i \right\rangle \qquad (3.16)$$

Making use of equation (3.11) and (3.13),equation (3.16)takes the form;

$$\left\langle \varphi_f \middle| U_f \frac{1}{E-H_f+i\varepsilon} W_f \frac{1}{E-H+i\varepsilon} V_i \middle| \varphi_i \right\rangle = \langle \varphi_f | U_f | \Psi_i^+ \rangle - \langle \varphi_f | U_f | \varphi_i \rangle -$$

$$\langle \chi_f^- | V_i | \varphi_i \rangle + \langle \varphi_f | V_i | \varphi_i \rangle \qquad (3.17)$$

Substituting equation (3.15) and (3.17) in equation (3.12),equation 3.18 is obtained;

$$T_{if} = \langle \varphi_f | V_f | \Psi_i^+ \rangle + \langle \chi_f^- | W_f | \Psi_i^+ \rangle - \langle \chi_f^- | W_f | \varphi_i \rangle + \langle \varphi_f | W_f | \varphi_i \rangle - \langle \varphi_f | U_f | \Psi_i^+ \rangle$$

$$+\langle \varphi_f | U_f | \varphi_i \rangle + \langle \chi_f^- | V_i | \varphi_i \rangle - \langle \varphi_f | V_i | \varphi_i \rangle \qquad (3.18)$$

Making use of the fact that on the energy shell;

$\langle \varphi_f | U_f + W_f | \varphi_i \rangle = \langle \varphi_f | V_f | \varphi_i \rangle = \langle \varphi_f | V_i | \varphi_i \rangle$equation(3.18) can be written as;

$$T_{if} = \langle \chi_f^- | V_i - W_f | \varphi_i \rangle + \langle \chi_f^- | W_f | \Psi_i^+ \rangle \qquad (3.19)$$

This is the two potential formula of Gillmann and Goldberger (Joachain,1975).

when$V_i = V_f = V$ and $W_f = V - U_f$ the T matrix can be re written as;

$$T_{if} = \langle \chi_f^- | U_f | \varphi_i \rangle + \langle \chi_f^- | W_f | \Psi_i^+ \rangle \qquad (3.20)$$

Here the wave function χ is distorted by the potential U according to equation 3.6. when U is chosen as some linear combination of static potentials of the target states, the first term on the right hand side of equation 3.20 vanishes for excitation process due to orthogonality of the target states and the T-matrix element reduces to equation 3.21;

$$T_{if} = \langle \chi_f^- | W_f | \Psi_i^+ \rangle \tag{3.21}$$

This is the model used to evaluate the scattering parameters and it is discussed in detail in chapter 4 with specific application to the electron impact excitation of the lowest autoionizing level of rubidium.

CHAPTER 4

METHODOLOGY

4.1 The Distorted wave method applied to electron-atom collision

The total Hamiltonian for the system of the scattering of an electron from a neutral atom is expressed as;

$$H = H_{\propto} - \frac{1}{2}\nabla_0^2 + V \tag{4.1}$$

where $H_{\propto}$ is the Hamiltonian for an isolated atom, the second term is the kinetic energy operator of an isolated projectile, V is the interaction between the projectile electron and the N-electron atom target and it is given by;

$$V = -\frac{N}{r_0} + \sum_{i=1}^{N} \frac{1}{r_{0i}} \tag{4.2}$$

Where $\frac{N}{r_0}$ and $\frac{1}{r_{01}}$ are the projectile electron target nucleus interaction term and projectileelectron target electron interaction term respectively.

The initial state full scattering wave function Ψ_i is a solution of schrödinger's equation;

$$(H - E)\Psi_i^+ = 0 \tag{4.3}$$

where the + sign indicates the outgoing wave boundary conditions. In this case, the projectile electron experiences either elastic or inelastic collision with an N electron atom, the exact T- matrix in the two potential approach is given by (Madison and Bartschat, 1996);

$$T_{if} = (N+1)\langle \chi_f^-(0)\psi_f(1,\dots,N)\big|V - U_f\big|A\Psi_i^+(0,\dots,N)\rangle +$$

$$\langle \chi_f^-(0)\psi_f(1,\dots,N)\big|U_f\big|\psi_i(1,\dots,N)\beta_i(0)\rangle \quad (4.4)$$

In the equation 4.4, ψ_i *and* ψ_f are the properly antisymmetrized initial and final atomicwave functions for the isolated atom, which diagonalizes the atomic Hamiltonian $H_\alpha$according to;

$$< \psi_{n'}|H_\alpha|\psi_n >= \varepsilon_n \delta_{nn'} \quad (4.5)$$

β_i is an initial state plane wave (eigen function for an isolated projectile) and A is the antisymmetrizing operator for the N+1 electrons. If $\Psi_i^+(0,\dots,N)$ is chosen to be a product of a projectile wave function and an antisymmetrized atomic wave function of electrons 1,… ,N, then antisymmetrization operator may be expressed as(Madison and Bartschat, 1996);

$$A = \frac{1}{N+1}(1 - \sum_{i=1}^{N} P_{i0}) \quad (4.6)$$

where theP_{i0} is the operator that exchanges electrons 0 and i. The potential U_f in equation (4.4) is an arbitrary distorting potential for the projectile, which is used to calculate χ_f^- by solving the equation;

$$\left(-\frac{1}{2}\nabla_0^2 - \frac{1}{2}k_f^2 + U_f\right)\chi_f^- = 0 \quad (4.7)$$

where the - superscript designates incoming wave boundary conditions and k_f is the final state wave vector of the projectile. Generally, the U_f*is* chosen to be any linear combination of initial and final state static potential of the target atom. In principle, however, U_f can be any potential as long as χ_f^- fulfils the appropriate boundary conditions. All the working shown above and in the equations below is in atomic

units. Forinelastic scattering, the second term in equation 4.4 vanishes for orthogonal atomic wavefunctions since U_f depends only on the single co-ordinate of the projectile. But for elastic scattering, the second term of the same equation is the dominant term, in fact it is generally the only contributing term since U_f is typically chosen such that the matrix elements of $V - U_f$ vanish.

The Lippmann Schwinger solution for Ψ_i^+ is given by;

$$\Psi_i^+ = [1 + G^+(V - U_i)]\psi_i\chi_i^+ \tag{4.8}$$

whereG^+ is the full Green's function given by;

$$G^+ = (E - H + i\eta)^{-1} \tag{4.9}$$

But since Ψ_i^+ cannot be evaluated without making approximations, in the distorted wave approach Ψ_i^+ is expressed in terms of a product of an initial state distorted wave χ_i^+ and an initial atomic wave function ψ_i in its first order approximation of equation (8).

Then equation 4.4 takes the form (for excitation process considered);

$$T_{if} = (N + 1)\langle\chi_f^-(0)\psi_f(1, \ldots, N)\big|V - U_f\big|A\chi_i^+(0)\Psi_i(1, \ldots., N)\rangle \tag{4.10}$$

The initial state distorted wave is a solution of the schrödinger's equation;

$$\left(-\tfrac{1}{2}\nabla_0^2 - \tfrac{1}{2}k_i^2 + U_i\right)\chi_i^+ = 0 \tag{4.11}$$

for an arbitrary distorting potential $U_i$which vanishes asymptotically.$k_i$is the incident wave vector and it is related to the incident energy by;

$$E_i = \tfrac{1}{2}\mathrm{k}_i^2 \tag{4.12}$$

4.2 Evaluation of Direct and Exchange Matrix Elements

Equation 4.13 shows the excitation process;

$$e^- + Rb\left[4p^6 5s^1,\ ^2S_{1/2}\right] \rightarrow e^- + Rb\left[4p^5 5s^2,\ ^2P_{1/2,3/2}\right] \tag{4.13}$$

where the 4p electron is excited to 5s. In the distorted wave approximation the transition matrices for the one electron system excited from an initial state *i*to a final state *f* by electron impact is expressed using atomic units as;

$$T^{dir} = \langle \chi_f^-(r_0)\psi_f(r_1)|V(r_0r_1)|\chi_i^+(r_0)\psi_i(r_1)\rangle \tag{4.14}$$

for direct excitation and;

$$T^{ex} = \langle \chi_f^-(r_0)\psi_f(r_1)|V(r_0r_1)|\chi_i^+(r_1)\psi_i(r_1)\rangle \tag{4.15}$$

for exchange excitation, where $V(r_0r_1)$ is the projectile-target atom interaction potential given by;

$$V(r_0, r_1) = z\left(\frac{1}{r_0} - \frac{1}{r_{01}}\right) \tag{4.16}$$

Where Z is the charge of the incident particle and is taken as -1 for the electron:r_0 is the position vector of the incident electron and r_1 is the position vector of an atomic electron undergoing a transition and r_{01} is the position vector between the projectile and target electron.

In order to evaluate the direct and exchange scattering amplitudes given above, the radial distorted waves$\chi_f^-$and $\chi_f^+$are expanded in terms of the partial waves as;

$$|\chi_f^+\rangle = \sqrt{\frac{2}{\pi}}\frac{1}{k_i r}\sum_{l_i m_i} i^{l_i}\chi_{l_i}(k_i, r)Y^*_{l_i m_i}(k_i) \tag{4.17}$$

and

$$|\chi_f^-\rangle = \sqrt{\frac{2}{\pi}}\frac{1}{k_f r}\sum_{l_f m_f} i^{l_f}\chi^*_{l_f}Y_{l_f m_f}Y^*_{l_f m_f}(k_f) \tag{4.18}$$

where$Y_{lm}$is a spherical harmonic.

In the expansion of χ_f^- the complex conjugate of radial part $\chi_{l_f}$and is taken so that it satisfies the incoming wave boundary conditions. Substituting the above partial wave expansion of the distorted waves in the equation 4.7 and equation4.11,it is found that the radial distorted waves are solutions of the following equation;

$$\left[\frac{d^2}{dr^2} - \frac{l_s(l_s+1)}{r^2} - U_s(r) + k_s^2\right]\chi_{ls}(r) = 0 \tag{4.19}$$

where s=i for initial state and s=f for the final state distorted wave. The equation (4.19) will be solved using Numerov's method. The differential cross section will be obtained using the relation;

$$\left(\frac{d\sigma}{d\Omega}\right)_{4p\to 5s} = \frac{1}{4\pi^2}\frac{k_f}{k_i}\sum_{m=-1}^{+1}\left[\frac{1}{4}\left|T^{dir}_{4p\to 5s} + T^{ex}_{4p\to 5s}\right|^2 + \frac{3}{4}\left|T^{dir}_{4p\to 5s} - T^{ex}_{4p\to 5s}\right|^2\right] \tag{4.20}$$

And the total cross section shall be obtained as;

$$\sigma = \int_0^{2\pi}\int_0^{\pi}\frac{d\sigma}{d\Omega}sin\theta d\theta d\phi \tag{4.21}$$

4.3 Distortion potential

A complex local spherically symmetric optical model potential for distortion of projectile wave have been used;

$$V_{opt}(r) = V_{st} + V_{exch} + iV_{abs} \quad (4.22)$$

whereV_{st} is the static potential,V_{exch} is a local energy dependent exchange potential and $iV_{abs}$is absorption potential arising because of the processes other than being considered i.e. because of absorption to other channels.

In this study the static potential of the target atom in its initial states as the distortion potential,$V_{st}$for the initial state of the projectile electron because, in initial state the projectile only 'sees' the initial state static potential of the target atom and a linear combination of the static potential of the target atom in its initial and final states as the distortion potential $V_{st}$for the final state of the projectile electron because when the energy of the projectile is transferred to the atom, it takes some time before the atom goes to its final state. Projectile in its final state 'sees' an intermediate potential between the initial and final state static potential of the target (Singh, 2004). That is;

$$U_i = \langle\psi_i|V|\psi_i\rangle = V_{st} \text{ in the initial channel} \quad (4.23)$$

$$U_f = \frac{1}{2}\langle\psi_i|V|\psi_i\rangle + \frac{1}{2}\langle\psi_f|V|\psi_f\rangle = V_{st} \text{ in the final channel} \quad (4.24)$$

Exchange potential of Furness and McCarthy (1973) is going to be used and it is given as;

$$V_{exc}(r) = \frac{1}{2}[E - V_{st}(r)] - \frac{1}{2}\{[E - V_{st}(r)]^2 + 4\pi\rho(r)\}^{1/2} \quad (4.25)$$

Absorption potential due to Staszewska*et al* (1984) given as;

$$V_{abs} = -\frac{1}{2}T_{loc}\rho(r)\sigma_b \quad (4.26)$$

where$T_{loc} = [2(E - V_{se})]^{1/2}$ is the local kinetic energy of the incident electron,$\rho(r)$is the electron charge density of the target atom, V_{se} is the static plus exchange potential and σ_b is the average binary collision cross section.

4.4 Evaluation of static potentials

The general mathematical formulation of static potentials is expressed as;

$$U_s = \langle \psi_s | V | \psi_s \rangle \tag{4.27}$$

whereψ_s is the target wave function s=i or f for initial or final state respectively and V is the interaction between the target and the projectile. HartreeFock wave functions of Clement and Roetti (1974) have been used for the target states. In these wave functions $\psi_s$is summed over slater type orbitals of the basis set as;

$$|\psi_s\rangle = \sum_n C_n |\phi_n\rangle \tag{4.28}$$

and

$$\langle \psi_s | = \sum_{n'} C^*_{n'} \langle \phi_{n'} | \tag{4.29}$$

The value of C_n represent the expansion coefficients and $\phi_n$are the slater type orbitals of the basis set. Using equation (4.27) and (4.28) in equation (4.29) the distortion potentials can be written as;

$$U_s = \sum_n \sum_{n'} C_n C^*_{n'} \langle \phi_{n'} | V | \phi_n \rangle \tag{4.30}$$

where V is the interaction potential in atomic units as given in equation (4.27). Since the target is being treated as one election atom, the interaction potential becomes;

$$V = -\frac{1}{r_0} + \frac{1}{r_{01}} \tag{4.31}$$

$\frac{1}{r_{01}}$can be expanded in spherical harmonics as;

$$\frac{1}{r_{01}} = \sum\sum \frac{4\pi}{2l+1} \frac{r_<^l}{r_>^{l+1}} Y_{l,m}(r_0) Y_{l,m}^*(r_1) \tag{4.32}$$

where$r_<$and$r_>$ are the lesser or greater of r_0 and r_1 respectively and $Y_{lm's}$ are spherical harmonics.

In distorted wave calculations, the spherically symmetric distorting potential used consists of the nuclear term on the right hand side of equation 4.31 plus the monopole term ($l=0$) of the summation of equation 4.32 since the effects of non-spherical terms is very small (Madison and Bartchat, 1996). Since;

$$Y_{0,0} = \frac{1}{\sqrt{4\pi}} \tag{4.33}$$

The static potential is thus expressed as (in Rydberg units);

$$U_s = 2\sum\sum C_n C_{n'}^* \left\langle \phi_{n'} \middle| \frac{1}{r_>} - \frac{1}{r_0} \middle| \phi_n \right\rangle \tag{4.34}$$

The slater type orbitals are expressed as a product of radial wave functions and spherical harmonics $Y_{l,m}$(Clementi and Roetti, (1974) and are given as;

$$\phi_n = N_n r^{\mu_n - 1} \exp(-\xi_n r) Y_{l,m}(\hat{r}) \tag{4.35}$$

where$\mu_n$is the principal quantum number of the n^{th} orbital of the basis set ξ is a constant and the normalization factor N_n of the orbital is given as;

$$N_n = \frac{(2\xi)^{\mu_n + \frac{1}{2}}}{\sqrt{(2\mu_n)!}} \tag{4.36}$$

When the values of the wave function are substituted in equation (4.35) and replace the Bra and Ket notation with the standard integrals a fully expanded static potential given below is obtained;

$$= 2\sum_{nlm}\sum_{n'l'm'} C_n C^*_{n'} N_n N^*_{n'} \int_{r_0}^{\infty} r_1^{\mu_n+\mu_{n'}} \left(\frac{1}{r_1}-\frac{1}{r_0}\right)\exp(-[\xi+\xi]r_1)dr_1 \int Y_{l,m}(r_0)Y_{l'm'}(r_1)\,d\Omega$$

(4.37)

In equation 4.37 above partial integration of the radial component is made use of such that from the radial distance 0, $r^0$is considered to be greater than r^1 while form r^0 to infinity isconsidered r^1 to be greater than r^0. Since the spherical harmonics are orthonormal, the last integral on the right hand side of equation4.37 vanishes unless $l=l'$ and $m=m'$

As a result the distortion potential reduces to;

$$U_s = \sum_{nn'lm} C_n C^*_{n'} N_n N^*_{n'} \int_{r_0}^{\infty} r_1^{\mu_n+\mu_{n'}} \left(\frac{1}{r_1}-\frac{1}{r_0}\right)\exp(-kr_1)dr_1 \qquad (4.38)$$

where$k = [\xi_n + \xi_{n'}]$ (4.39)

In this case the integral above 4.38 was evaluated analytically in order to get the exact static potentials which have been used as the distortion potentials. The analytical solutions of equation 4.38 depends on the sum of the principal quantum numbers,$\mu_n$and $\mu_{n'}$ and the sum varies from 2 to 10 for the problem that was solved.

Table 4.1 Analytical solutions.

$\mu_n + \mu_{n'}$	Distortion potential elements form$\langle n'\|U_s\|n\rangle$
2	-const(n,n')x$(X+2!)e^{-x}$
3	-const(n,n')x$(X^2+4X+3!)e^{-x}$
4	-const(n,n')x$(X^3+6X^2+18X+4!)e^{-x}$
5	-const(n,n')x$(X^4+8X^3+36X^2+96X+5!)e^{-x}$
6	-const(n,n')x$(X^5+10X^4+60X^3+240X^2+600X+6!)e^{-x}$
7	-const(n,n')x$(X^6+12X^5+90X^4+480X^3+1800X^2+4320X+7!)e^{-x}$
8	-const(n,n')x$(X^7+14X^6+126X^5+840X^4+4200X^3+15120X^2+35280X+8!)e^{-x}$
9	-const(n,n')x$(X^8+16X^7+168X^6+1344X^5+8400X^4+40320X^3+141120X^2+322560X+9!)e^{-x}$
10	-const(n,n')x$(X^9+18X^8+216X^7+2016X^6+15120X^5+90720X^4+423360X^3+1451520X^2+3265920X+10!)e^{-x}$

In table 4.1

$$X = (\xi_n + \xi_{n'})r_0$$

And $const(n,n') = \frac{C_n C_{n'} N_n N_{n'}}{X r_0}$ since the values of C_n,ξ_n and μ_n are obtained from the atomic data tables for the atomic wave functions compiled by Clementi and Roetti,(1974),it was possible to write a computer program to sum the various matrix elements accurately to generate the desired static potential.

4.5 Angular correlation parameters $\lambda$and A_{20}

$\lambda$is calculated using the relation(Kaur and Srivastava, 1999);

$$\lambda = \frac{\sigma_0(\theta,\phi)}{\sigma_0(\theta,\phi)+2\sigma_1(\theta,\phi)} 0 \leq \lambda \leq 1 \quad (4.40)$$

and

$$A_{20} = \frac{\sigma_1 - \sigma_0}{\sigma} \quad (4.41)$$

where$\sigma_0(\theta,\phi)$and $\sigma_1(\theta,\phi)$ are the differential cross sections for $np_m \rightarrow (n+1)s$ transition with $m = 0\ and\ 1$ respectively and are related to their scattering amplitude $f_m\ (\theta,\phi)$ by;

$$\sigma_m(\theta,\phi) = \frac{k_f}{k_i}|f_m(\theta,\phi)|^2 \quad (4.42)$$

Hereσ_0 and $\sigma_1$give the total cross section for the magnetic sublevels 0 and 1 respectively while the scattering amplitude is directly connected to the transition matrix using the relation;

$$f_m(\theta,\phi) = -\frac{1}{2\pi}T_{if}(m) \quad (4.43)$$

Where$T_{if}(m)$ is the T matrix for the excitation process.

4.6 Atomic wave functions

The atomic wave functions which were used were based on Rootham-Hartee-Fock expansion technique and the multi zeta functions as given in the Clementi and Roetti (1974) tables. A single zeta function is an approximation function in which a given electron orbital is described by one Slater functions while a multi zeta functions is an approximation of the RHF where a given electron orbital is described by many Slater function as shown in equation 4.44;

$$\Psi = \mathrm{A}(\Phi_1^{(1)} \ldots\ldots\ldots \Phi_n^{(n)} \quad (4.44)$$

Where A is the antisymmetrizing operator , n is the total number of electrons and $\Phi_1^{(1)} \ldots\ldots\ldots \Phi_n^{(n)}$ are the spin orbitals (one electron functions).

The spin orbital is simply a product of a spin function and an orbital function. The orbitals are assumed to be orthogonal to each other thus the same holds for spin orbitals. The orbitals are obtained by solving the RHT equations. The target wave function is considered as one electron wave function and so the specific spin orbital wave function were used in the transition matrix as the bound state target wave function.

The orbitals are characterized by an index,η,which indicates the symmetry species (η, corresponds to the orbital quantum number l), by an index,α,which indicates the subspecies. These subspecies label individual members of the degenerate set that standform according to the representation ηalso characterizes the orbitals. The orbital $\Phi_{i\eta\alpha}$is expanded in terms of the basis functions according to;

$$\Phi_{i\eta\alpha} = \sum_p \Phi_{p\eta\alpha} C_{i\eta p}$$

(4.45)

where p is the p^{th}basis function of the symmetry, the coefficients depend on i, η and p but notα. The basis functons $\Phi_{p\eta\alpha}$ are Slater type orbitals with integer quantum numbers,

namely;

$$\Phi_{p\eta\alpha}(r\theta\phi) = R_{\eta p}(r) Y_{\eta\alpha}(\theta\phi) \qquad (4.46)$$

where;

$$R_{\eta p}(r) = \left[(2\mu_{\eta p}\right]^{1/2} (2\xi_{\eta p})^{\mu_{\eta p}+1/2} r^{n_{\eta p}-1} e^{-\xi_{\eta p} r} \qquad (4.47)$$

And $Y_{\eta\alpha}(\theta\phi)$ are normalized spherical harmonics in complex form. It is noted that $\mu_{\eta p} \geq \eta + 1$and the exponent $\xi_{\eta p}$ is chosen so as to give the best energy found by laborious process of optimization (Clementi and Roetti,1974).

The single electron wave functions shown in $\Phi_{i\eta\alpha} = \sum_p \Phi_{p\eta\alpha} C_{i\eta p}$is then constructed using the table of coefficients as the exponents for the radial part of equation 4.46 provided in the atomic data tables of Clementi and Roetti,(1974). The multi zeta type wave functions for rubidium ($4p^5 5s^2$) are given as;

$$\Phi(5s) = 0.00066\phi_1 + 0.01390\phi_2 + 0.02262\phi_3 - 0.07316\phi_4 + 0.02802\phi_5$$

$$+0.08360\phi_6 - 0.14618\phi_7 - 0.11134\phi_8 + 0.12653\phi_9 + 0.53476\phi_{10}$$

$$+ 0.46820\phi_{11}$$

$$\Phi(4p) = 0.00899\phi_{12} + 0.128997\phi_{13} - 0.22816\phi_{14} - 0.16836\phi_{15} + 0.47521\phi_{16}$$

$$+0.55302\phi_{17} + 0.11614\phi_{18}$$

where;

$$\phi_1 = N_1 r^0 \exp(-38.058920r) Y_{0,0}(\theta\phi)$$

$$\phi_2 = N_2 r^0 \exp(-26.1789r) Y_{0,0}(\theta\phi)$$

$$\phi_3 = N_3 r^1 \exp(-17.87590r) Y_{0,0}(\theta\phi)$$

$$\phi_4 = N_4 r^1 \exp(-15.13760r) Y_{0,0}(\theta\phi)$$

$$\phi_5 = N_5 r^2 \exp(-9.32726r) Y_{0,0}(\theta\phi)$$

$$\phi_6 = N_6 r^2 \exp(-6.80548r) Y_{0,0}(\theta\phi)$$

$\phi_7 = N_7 r^3 \exp(-3.91418r) Y_{0,0}(\theta\phi)$

$\phi_8 = N_8 r^3 \exp(-2.58977r) Y_{0,0}(\theta\phi)$

$\phi_9 = N_9 r^4 \exp(-1.88043r) Y_{0,0}(\theta\phi)$

$\phi_{10} = N_{10} r^4 \exp(-1.15468r) Y_{0,0}(\theta\phi)$

$\phi_{11} = N_{11} r^4 \exp(-0.74153r) Y_{0,0}(\theta\phi)$

$\phi_{12} = N_{12} r^1 \exp(-24.44350r) Y_{1,p}(\theta\phi)$

$\phi_{13} = N_{13} r^1 \exp(-15.28570r)\, Y_{1,p}(\theta\phi)$

$\phi_{14} = N_{14} r^2 \exp(-8.24457r) Y_{1,p}(\theta\phi)$

$\phi_{15} = N_{15} r^2 \exp(-5.69739r) Y_{1,p}(\theta\phi)$

$\phi_{16} = N_{16} r^3 \exp(-3.64326r) Y_{1,p}(\theta\phi)$

$\phi_{17} = N_{17} r^3 \exp(-2.33347r) Y_{1,p}(\theta\phi)$

$\phi_{18} = N_{18} r^3 \exp(-1.56570r) Y_{1,p}(\theta\phi)$

And the normalization factors are given as $N_1 = 469.5851382$,$N_2 = 267.8903606$,

$N_3 = 1560.052305$, $N_4 = 1029.4465818$, $N_5 = 1044.907935$,$N_6 = 346.6924657$,

$N_7 = 52.33091033$, $N_8 = 8.157368834$, $N_9 = 0.765945557$, $N_{10} = 0.052398939$

$N_{11} = 0.004586606184, N_{12} = 3410.969586,\ N_{13} = 1054.830546,\ N_{14} = 678.4639408$

$N_{15} = 186.1249345, N_{16} = 37.89487371,\ N_{17} = 5.10369504$ and $N_{18} = 0.847350716$

4.7 Computer program DWBA1

To evaluate the various physical parameters, differential cross section and integral cross section, $\lambda$and A_{20} parameters, the modified form of an existing computer program developed by Madison and Bartschat (1996) which is in Fortran language was used.

Thefollowing modifications were done to generate the data presented;

- The main program, has been modified to generate cross sections for energies upto 1000eV and to calculate lambda and alignment parameters.
- In addition, in the main program the *s-p* target electron transition was changed to cater for *p-s* transition, that is, *4p-5s*. This involved changing angular momentum parameters such as orbital and magnetic quantum numbers.
- The subroutine FHYD for hydrogen wave functions was modified to generate rubidiumwave functions for 4p and 5s states.
- The subroutine POTENT for hydrogen static potentials was modified to generate static, static plus exchange and static plus exchange plus absorption potentials ascomplex distortion potentials for rubidium atom

In order to perform data analysis, Origin 8 Lab was used to represent the data graphically.

CHAPTER 5

RESULTS AND DISCUSSION

5.1 Introduction

In this chapter the distorted wave method results for integral and differential cross section for inelastic scattering of electrons by a rubidium atom have been presented. The present results (with static potential, static plus exchange potential, static plus exchange plus absorption potential) have been compared amongst themselves and with the available experimental and calculated results. Multi zeta (MZ) wave functions have been used in this work. The results have been compared with those of Pangantiwar and Srivastava (1987), Borovik *et al.* (2012) and Borovik*et al.* (2013) for electron impact excitation of the lowest autoionizing state of rubidium. The result for Borovik*et al.* (2012) was obtained through experiment, Borovik*et al.(*2013) was obtained theoretically by employing a fully relativistic Dirac B-spline R-matrix (close-coupling) model and for Pangantiwar and Srivastava (1987) results is a calculation using the distorted wave method where the initial state static potential is the initial channel distortion potential while the final state static potential is the final channel distortion potential.

5.2 Integral Cross Sections

In this study integral cross sections (ICS) for inelastic scattering of electrons by a rubidium atom were calculated at the range of 15.8 –1000 eV. Table 5.1 gives the present inelastic integral cross sections, obtained using static potential, static plus exchange potential and static plus exchange plus absorption potential. The present

integral cross sections results for electron impact excitation of the $4p^5 5s^2$state of Rubidium are compared with the works ofPangantiwar and Srivastava (1987), Borovik*et al.* (2012) and Borovik*et al.* (2013) in figure 5.1.

The present integral cross section results indicate that when only static potential is taken as the distortion potential, it gives larger cross sections compared to those obtained when static plus exchange and static plus exchange plus absorption potentials are used as distortion potential. This study also reveals that with absorption potential the cross sections are lowered compared to when only exchange potential is included in the distortion potential.

At lower energies between 15.8-18.6eV and at energies above 50eV the present three sets of cross sections are nearly the same. Energies between 19.0 – 50eV the cross sections are so different with static potential results having the highest cross sections followed by static plus exchange andstatic plus exchange plus absorption potential results having the lowest values. This can be attributed to the opening of several or an infinite number of channels in addition to the elastic channel.

It is also clear that there is an abrupt increase in the integral cross sections at electron energy just above threshold energy of the lowest autonizing state of rubidium and it peaks at about 18.6eV. This is due to formation of a composite state of negative ion Rb^- which then decays into the rubidium atom in the autoionizing state and a free scattered electron with low energy which explain a sharp increase in the cross section near threshold energy.It can also be as a result of exchange effects between projectile electron and atomic electron at low impact energies.

From 19 to 50eV the effect of exchange and absorption potential is very much apparent, with the absorption potential lowering the cross section much more than exchange potential and brings the cross section closer to the experimental results of Borovik *et al.* (2012). And this is due to the opening of more channels at this point and considerable amount of time spent by the incident electron in the vicinity of the atom.

At higher projectile energies the effects of exchange and absorption potentials are not visible and that`s why the present three sets of cross section results are nearly equal. This is due to the less interaction between the projectile electron and the target atom.

The present result for energies greater than 50eV are slightly higher than those of Pangantiwar and Srivastava (1987), this can be due to the choice of distortion potential. In the present calculation we have applied as proposed by Singh (2004), initial state static potential as the initial channel distortion potential while a linear combination of initial and final state static potentials as the final channel distortion potential while in Pangantiwar and Srivastavacalculation initial state static potential is the initial channel distortion potential while the final state static potential is the final channel distortion potential. In addition, it could be attributed to the present results as we applied MZ Hartree fork wave functions by Clementi and Roetti (1974) while they used MZ Hartree fork wave functions by Clementi*et al.* (1967)

When compared with Borovik*et al.* (2012) and Borovik*et al.* (2013) results they are in good agreement with both experimental and theoretical results. Near threshold there is a sharp rise in the cross sections, though the peak in the present result shifts toward the right.

Table 5.1Integral cross sections for electron impact excitation of $4p^5 5s^2$ state of rubidium atom

Energy (eV)	Static potential	Static and exchange Potential	Static ,exchange and absorption potential
15.8	5.962E-03	8.61E-03	8.61E-03
15.9	2.146E-03	2.94E-02	2.94E-02
16	4.233E-03	5.61E-02	5.61E-02
17	3.191E-01	3.46E-01	3.46E-01
18	4.491E-01	4.53E-01	4.53E-01
18.2	4.565E-01	4.58E-01	4.58E-01
18.4	4.601E-01	4.59E-01	4.59E-01
18.6	4.603E-01	4.58E-01	4.58E-01
18.8	4.578E-01	4.54E-01	4.54E-01
19	4.533E-01	4.49E-01	4.49E-01
20	4.141E-01	4.08E-01	4.08E-01
30	2.475E-01	2.49E-01	1.53E-01
40	2.883E-01	2.89E-01	2.37E-01
50	2.980E-01	2.98E-01	2.90E-01
60	2.920E-01	2.92E-01	2.86E-01
80	2.733E-01	2.73E-01	2.69E-01
100	2.567E-01	2.57E-01	2.54E-01
200	1.936E-01	1.94E-01	1.93E-01
400	1.312E-01	1.31E-01	1.31E-01
600	1.002E-01	9.83E-02	9.82E-02
800	7.511E-02	7.50E-02	7.50E-02
1000	5.971E-02	5.93E-02	5.93E-02

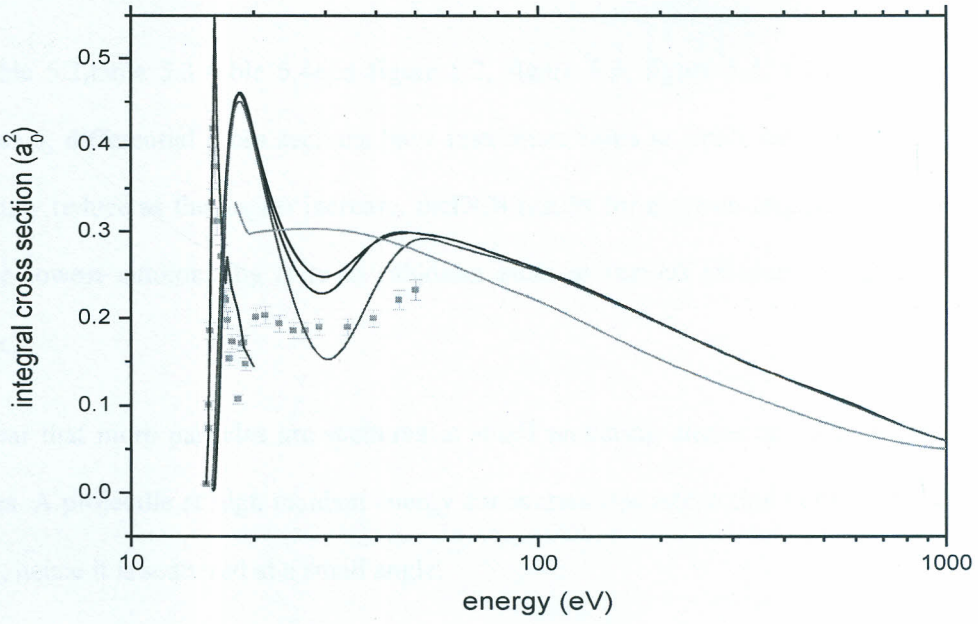

figure 5.1. Intergral cross section for excitation of the lowest autoionising level in rubidium;

——— present static

———present static and exchange

———present static , exchange and absorption

——— Srivastava and Pangantiwar (1987)

———Borovik theoretical (2012)

▪ Borovik experimental (2013)

5.2 Differential Cross Sections

In table 5.2,table 5.3 table 5.4and figure 5.2, figure 5.3, figure 5.4, figure 5.5 and figure5.6, differential cross sections have maximum value at small scattering angles and they reduce as the angles increase. theDCS results for electron impact excitation of the lowest autoionizing state in rubidium atom at various incident energies are given.

Is clear that more particles are scattered at small scattering angles and less at large angles. A projectile at high incident energy encounters less interaction with the target atom, hence it is scattered at a small angle.

The differential cross section results for 30 and 50eV electron impact energies (Figure 5.4 and Figure 5.5) obtained using absorption potential are lower compared to the ones obtained with static and exchange potentials. This is because at these energies more channels are open and the potentials have more time to show their effects (since velocity of the projectile is not very high). At energies lower than 30eV less channels are open hence absorption potential has little effect and at energies greater than 50Ev the time spent by the projectile in the vicinity of the target atom is less so the effect of the potentials are little.

When compared to the Pangantiwar and Srivastava (1978) results , the present DCS results show the same trend as the Pangantiwar and Srivastava`s results. Variations at low energies can be attributed to the different choices in the distortion potential. No experimental results for differential cross sections are available for comparison.

Differential cross sections for electron impact using static potential are larger at all angles compared to those of of static and exchange and static, exchange and

absorption potentials.And this observation is more visible near excitation threshold. This is because at energies near excitation threshold, there is more interaction of the projectile electron with the target electrons due to attraction by the positive nucleus compared to larger energies.

The study can also be justified by comparing DCS in this study and the study of Pangantiwar and Srivastava (1987) which have a similar trend at different angles even with increase in energy, but slight variations are due to the different type of distortion potential chosen. differential cross section

Table 5.2.Present differential cross sections results for electron impact excitation of the lowest autoionizing state in rubidium atom at various incident energies of the projectile using static potential

Scattering Angle(deg)	Incident projectile energy (eV)				
	17	20	30	50	100
0	2.64E-02	1.60E-01	8.57E-01	2.76E+00	7.80E+00
10	2.37E-02	1.36E-01	5.59E-01	9.33E-01	6.26E-01
20	1.73E-02	8.36E-02	1.88E-01	1.21E-01	1.22E-02
30	1.06E-02	3.95E-02	4.37E-02	1.09E-02	6.21E-03
40	5.84E-03	1.64E-02	1.15E-02	7.39E-03	5.06E-03
50	3.55E-03	8.42E-03	8.11E-03	7.65E-03	2.15E-03
60	3.02E-03	6.77E-03	7.93E-03	5.42E-03	8.13E-04
80	3.01E-03	5.79E-03	5.11E-03	1.80E-03	2.00E-04
100	1.90E-03	3.72E-03	2.40E-03.	6.21E-04	9.89E-05
120	1.79E-03	2.89E-03	1.00E-03	3.02E-04	5.86E-05
140	4.53E-03	3.92E-03	4.05E-04	2.16E-04	3.56E-05
160	8.48E-03	5.60E-03	1.92E-04	1.98E-04	2.28E-05
180	1.03E-02	6.37E-03	1.30E-04	1.96E-04	1.82E-05

Table 5.3.Present differential cross sections results for electron impact excitation of the lowest autoionizing state in rubidium atom at various incident energies of the projectile using static and exchange potential

Scattering Angle(deg)	Incident projectile energy (eV)				
	17	20	30	50	100
0	2.88E-02	1.61E-01	8.56E-01	2.76E+00	7.80E+00
10	2.59E-02	1.37E-01	5.58E-01	9.32E-01	6.26E-01
20	1.90E-02	8.42E-02	1.88E-01	1.21E-01	1.22E-02
30	1.17E-02	4.00E-02	4.41E-02	1.11E-02	6.25E-03
40	6.47E-03	1.68E-02	1.19E-02	7.54E-03	5.08E-03
50	3.97E-03	8.73E-03	8.40E-03	7.74E-03	2.15E-03
60.	3.40E-03	7.05E-03	8.13E-03	5.46E-03	8.13E-04
80	3.42E-03	5.99E-03	5.20E-03	1.82E-03	2.00E-04
100	2.17E-03	3.86E-03	2.45E-03	6.27E-04	9.88E-05
120	2.02E-03	2.99E-03	1.02E-03	3.05E-04	5.84E-05
140	5.11E-03	3.98E-03	4.13E-04	2.19E-04	3.55E-05
160	9.62E-03	5.62E-03	1.95E-04	2.02E-04	2.25E-05
180	1.17E-02	6.39E-03	1.32E-04	2.01E-04	1.81E-05

Table 5.4.Present differential cross sections results for electron impact excitation of the lowest autoionizing state in rubidium atom at various incident energies of the projectile using static, exchange and absorption potential

Scattering Angle(deg)	Incident projectile energy (eV)				
	17	20	30	50	100
0	2.88E-02	1.61E-01	5.02E-01	2.77E+00	7.75E+00
10	2.59E-02	1.37E-01	3.08E-01	9.31E-01	6.19E-01
20	1.90E-02	8.42E-02	8.83E-02	1.16E-01	1.21E-02
30	1.17E-02	4.00E-02	1.93E-02	7.21E-03	6.28E-03
40	6.47E-03	1.68E-02	7.85E-03	5.31E-03	4.93E-03
50	3.97E-03	8.73E-03	5.81E-03	6.46E-03	2.01E-03
60	3.40E-03	7.05E-03	4.24E-03	4.66E-03	7.19E-04
80	3.42E-03	5.99E-03	1.42E-03	1.36E-03	1.68E-04
100	2.17E-03	3.86E-03	1.66E-04	3.36E-04	8.91E-05
120	2.02E-03	2.99E-03	3.11E-04	1.22E-04	5.52E-05
140	5.11E-03	3.98E-03	3.40E-04	9.44E-05	3.33E-05
160	9.62E-03	5.62E-03	1.82E-04	9.83E-05	2.05E-05
180	1.17E-02	6.39E-03	1.13E-04	1.01E-04	1.57E-05

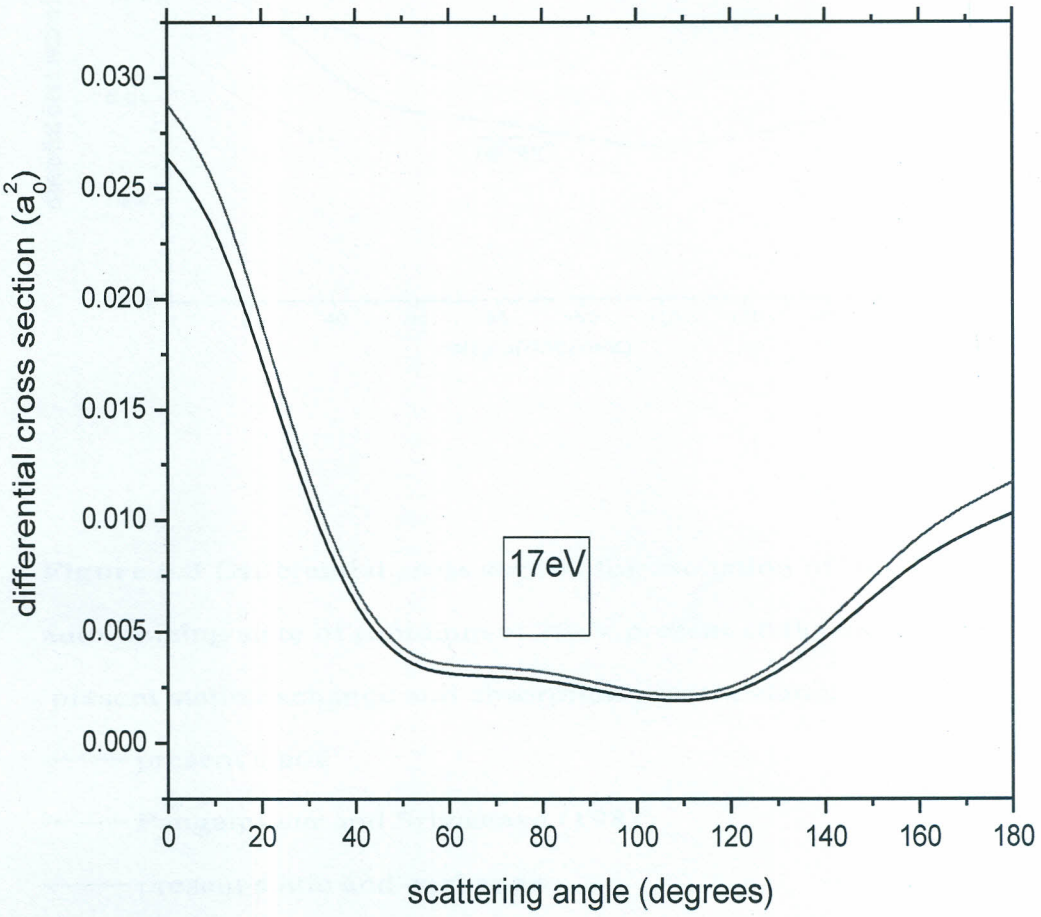

Figure 5.2 Differential cross section for excitation of the lowest autoionizing state of rubidium at 17eV

—— present static and exchange

—— present static,exchange and absorption

—— present static

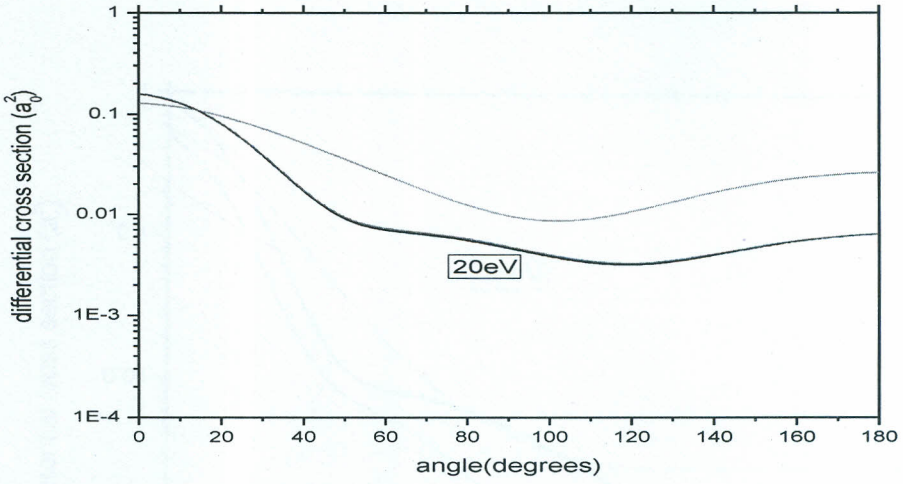

Figure 5.3 Differential cross section for excitation of the lowest autoionizing state of rubidium at 20eV present static and exchange present static,exchange and absorption present static;

——— present static

——— Pangantiwar and Srivastava (1987)

——— present static and exchange

——— present static,exchange and absorption

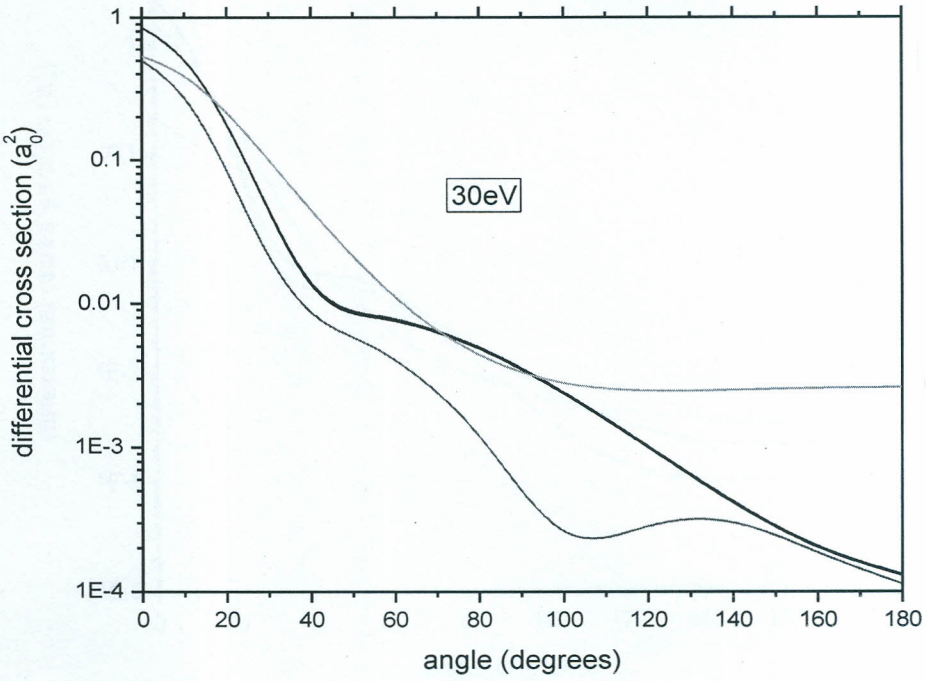

Figure 5.4. Differential cross section for excitation of the autoionizing state in rubidium at 30eV;

—— present static potential distortion potential results

—— present static and exchange distortion potential results

—— Pangantiwar and Srivastava (1987) results

—— present static,exchange and absorption distortion potential results

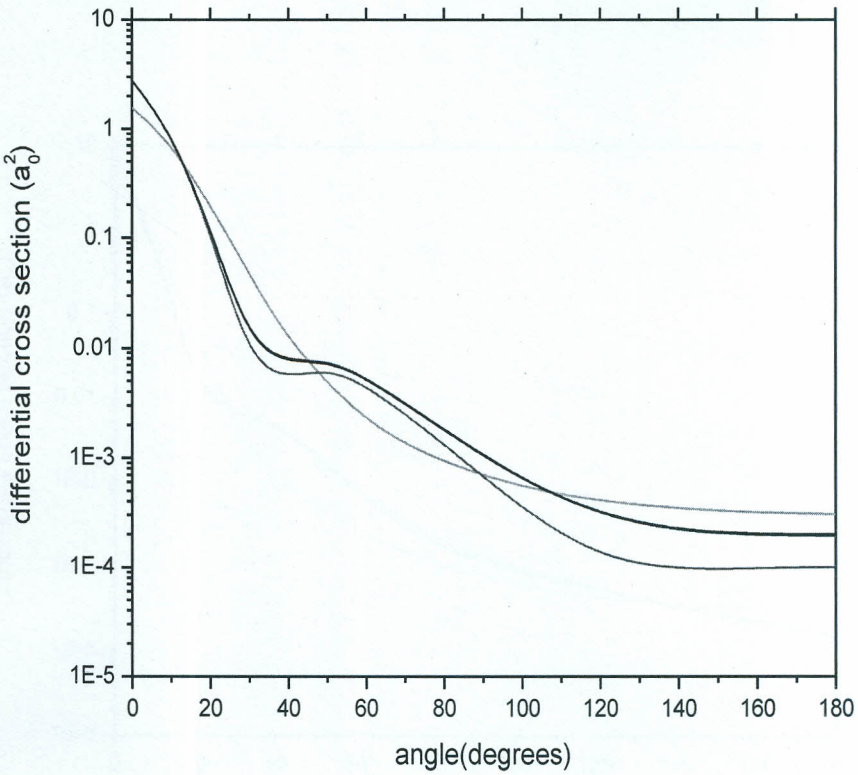

Figure 5.5. Differential cross section for excitation of the autoionizing state in rubidium at 50eV;

—— Pangantiwar and Srivastava (1987)

—— present static

—— present static,exchange and absorption

—— present static and exchange

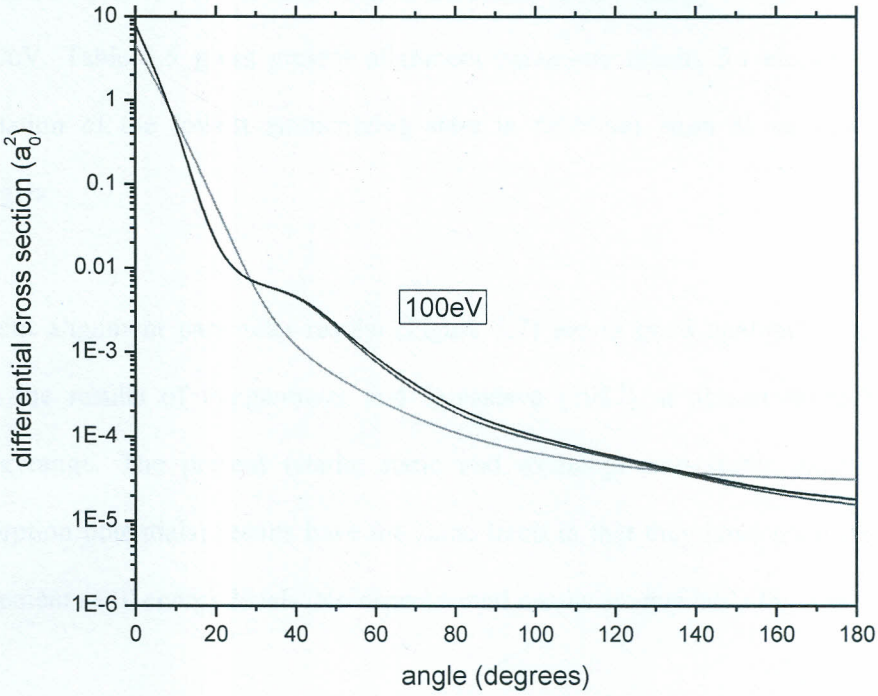

Figure 5.6. Differential cross section for excitation of the autoionizing state in rubidium at 100eV;

——Pangantiwar and Srivastava (1987)

—— present static

—— present ststic ,exchange and absorption

—— present static and exchange

5.3 Alignment parameter

The present alignment parameter result is compared with the work of Pangantiwar and Srivastava (1987) for electron impact excitation at an energy range of 15.8eV to 1000eV. Table 5.5 gives present alignment parameter results for electron impact excitation of the lowest autoionizing state in rubidium atom at various incident energies.

Present alignment parameter results (Figure 5.7) are in good qualitative agreement with the results of Pangantiwar and Srivastava (1987) at almost throughout the energyrange. The present (static, static and exchange and static, exchange and absorption potentials) results have the same trend in that they have good qualitative agreement at all energy levels. No experimental results are available for comparison.

Specifically, the result for static, exchange and absorption potential results have a better agreement with Pangantiwar and Srivastava (1987) in terms of the pattern and trend of the graph achieved, Pangantiwar and Srivastava (1987) results are slightly lower in comparison and this may be attributed to the choice of their distortion potential (initial- and final-state static potentials used for distorting the incident and scattered projectile electron).

It is noted that the results alignment parameter do not agree among themselves at energies near excitation threshold due to large effect of the interaction potential since interaction time is large. The three results tend to converge at higher energies similar

to the results for integral cross sections, since the effect of different distortion potentials will not be so apparent.

It is also worth noting that from the formula for the alignment parameter, if A_{20} is negative, then $\sigma_0 > \sigma_1$ implying that the excitations are aligned more to the magnetic sub-state m=0 compared to the magnetic sub-state m=1. Otherwise, when A_{20} is positive, i.e. $\sigma_1 > \sigma_0$, excitoations are aligned more to the m=1 level. From the figure it is seen that for impact energies up to 300eV, $\sigma_0 > \sigma_1$ and above that $\sigma_1 > \sigma_0$.

Table 5.5. Present alignment parameter results for electron impact excitation of the lowest autoionizing state in rubidium atom at various incident energies.

Energy (eV)	Static potential	Static and exchange Potential	Static ,exchange and absorption potential
15.8	-7.60E-01	-7.80E-01	-7.80E-01
15.9	-6.54E-01	-6.56E-01	-6.56E-01
16	-6.06E-01	-6.03E-01	-6.03E-01
17	-5.26E-01	-5.25E-01	-5.25E-01
18	-5.08E-01	-5.07E-01	-5.07E-01
18.2	-5.04E-01	-5.02E-01	-5.02E-01
18.4	-5.01E-01	-5.00E-01	-5.00E-01
18.6	-4.98E-01	-4.97E-01	-4.97E-01
18.8	-4.94E-01	-4.93E-01	-4.93E-01
19	-4.90E-01	-4.89E-01	-4.89E-01
20	-4.75E-01	-4.73E-01	-4.73E-01
30	-3.71E-01	-3.71E-01	-2.61E-01
40	-3.14E-01	-3.14E-01	-2.80E-01
50	-2.75E-01	-2.75E-01	-2.68E-01
60	-2.43E-01	-2.43E-01	-2.39E-01
80	-1.93E-01	-1.93E-01	-1.91E-01
100	-1.59E-01	-1.59E-01	-1.56E-01
200	-6.40E-02	-6.40E-02	-6.26E-02
400	4.61E-02	4.61E-02	4.66E-02
600	1.77E-01	1.77E-01	1.77E-01
800	2.61E-01	2.61E-01	2.62E-01
1000	3.28E-01	3.28E-01	3.29E-01

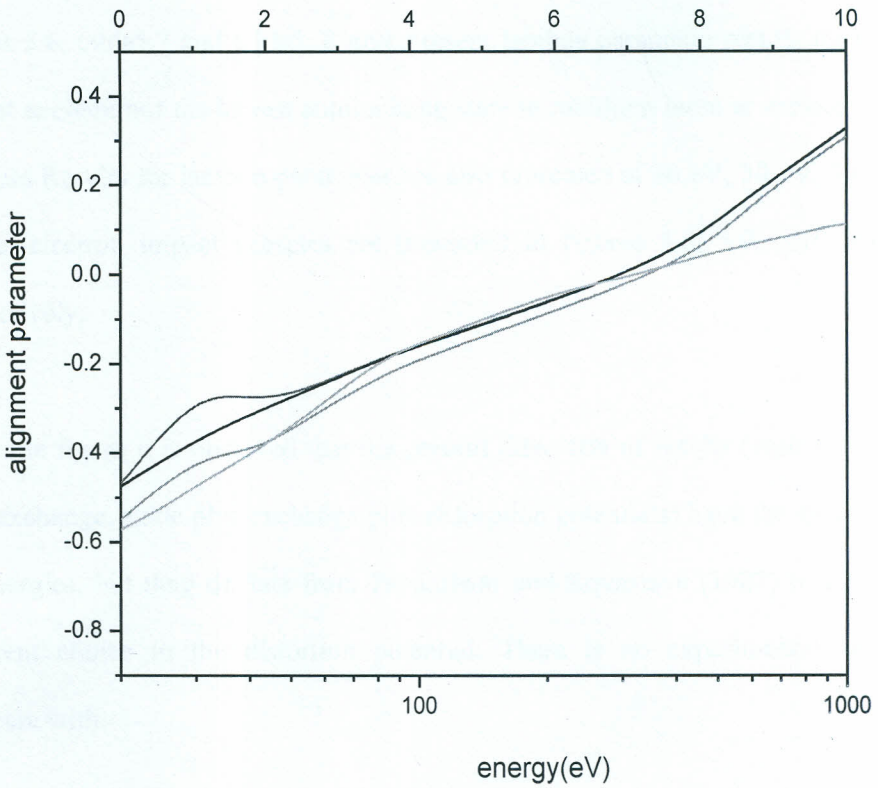

Figure 5.7.Present alignment parameter results for electron impact excitation of the lowest autoionizing state in rubidium atom at various incident energies;

—— present static ,exchange and absorption

—— present static and exchange

—— present static

——Pangantiwar and Srivastavar (1987)

—— Kaur and Srivastava (1999)

5.4 Lambda parameter λ

Tables 5.6, table5.7 and table5. 8 give present lambda parameter results for electron impact excitationof the lowest autoionizing state in rubidium atom at various incident energies.Results for lambda parameter are also presented at 20 eV, 30 eV, 50 eV and 100 eVelectron impact energies are presented in figures 5.8, 5.9, 5.10 and 5.11 respectively.

From the figure it is observed that the present three sets of results (with static, static plus exchange, static plus exchange plus absorption potentials) have the same trend at all energies, but they deviate from Pagantiwar and Srivastava (1987) results due to different choice in the distortion potential. There is no experimental results to compare with.

It is also worth noting that at the small and large angles closer to 0^0 and 180^0, particles are scattered more to the magnetic sub-state m=0 since from the formula, it is clear that for $\lambda=1$, $\sigma_0 \gg \sigma_1$. At intermediate angles σ_0 decreases and σ_1 increases, but still in most cases $\sigma_0 > \sigma_1$.

Table 5.6. Present lambda parameter results for electron impact excitation of the lowest autoionizing state in rubidium atom at various incident energies of the projectile using static potential.

Scattering Angle(deg)	Incident projectile energy (eV)				
	17	20	30	50	100
0	1.00E+00	1.00E+00	1.00E+00	1.00E+00	1.00E+00
10	9.60E-01	9.33E-01	7.93E-01	4.93E-01	1.34E-01
20	8.32E-01	7.45E-01	4.17E-01	1.36E-01	3.54E-01
30	6.01E-01	4.77E-01	2.31E-01	6.78E-01	2.36E-01
40	2.97E-01	2.79E-01	7.07E-01	5.53E-01	6.45E-02
50	2.05E-01	5.05E-01	8.37E-01	1.68E-01	5.94E-02
60	5.64E-01	8.80E-01	4.56E-01	5.96E-02	8.04E-02
80	9.94E-01	7.33E-01	7.14E-02	2.33E-02	1.82E-01
100	5.57E-01	2.02E-01	9.26E-04	4.68E-02	2.91E-01
120	6.73E-02	6.88E-02	1.07E-02	2.41E-01	3.79E-01
140	6.94E-01	5.99E-01	1.15E-01	6.14E-01	5.36E-01
160	9.44E-01	9.18E-01	5.76E-01	9.05E-01	8.14E-01
180	1.00E+00	1.00E+00	9.98E-01	1.00E+00	9.98E-01

Table 5.7.Present lambda parameter results for electron impact excitation of the lowest autoionizing state in rubidium atom at various incident energies of the projectile using static and exchange potential.

Scattering Angle(deg)	Incident projectile energy (eV)				
	17	20	30	50	100
0	1.00E+00	1.00E+00	1.00E+00	1.00E+00	1.00E+00
10	9.60E-01	9.33E-01	7.93E-01	4.92E-01	1.34E-01
20	8.33E-01	7.45E-01	4.17E-01	1.39E-01	3.59E-01
30	6.02E-01	4.78E-01	2.40E-01	6.87E-01	2.37E-01
40	3.01E-01	2.90E-01	7.21E-01	5.55E-01	6.50E-02
50	2.10E-01	5.22E-01	8.35E-01	1.70E-01	5.90E-02
60	5.63E-01	8.82E-01	4.55E-01	6.02E-02	7.96E-02
80	9.92E-01	7.25E-01	7.08E-02	2.23E-02	1.83E-01
100	5.64E-01	2.00E-01	1.82E-03	4.67E-02	2.94E-01
120	5.93E-02	6.76E-02	6.71E-03	2.45E-01	3.79E-01
140	6.87E-01	5.91E-01	9.74E-02	6.19E-01	5.34E-01
160	9.43E-01	9.15E-01	5.61E-01	9.07E-01	8.12E-01
180	1.00E+00	1.00E+00	9.98E-01	1.00E+00	9.98E-01

Table 5.8.Present lambda parameter results for electron impact excitation of the lowest autoionizing state in rubidium atom at various incident energies of the projectile using static, exchange and absorption potential.

Scattering Angle(deg)	Incident projectile energy (eV)				
	17	20	30	50	100
0	1.00E+00	1.00E+00	1.00E+00	1.00E+00	1.00E+00
10	9.60E-01	9.33E-01	6.92E-01	4.92E-01	1.28E-01
20	8.33E-01	7.45E-01	1.36E-01	1.00E-01	3.75E-01
30	6.02E-01	4.78E-01	2.38E-01	5.09E-01	2.39E-01
40	3.01E-01	2.90E-01	9.44E-01	4.12E-01	5.89E-02
50	2.10E-01	5.22E-01	4.06E-01	8.38E-02	4.95E-02
60	5.63E-01	8.82E-01	8.60E-03	2.33E-02	6.57E-02
80	9.92E-01	7.25E-01	5.08E-01	2.98E-02	1.78E-01
100	5.64E-01	2.00E-01	8.39E-01	5.80E-02	3.06E-01
120	5.93E-02	6.76E-02	9.48E-01	3.89E-01	3.87E-01
140	6.87E-01	5.91E-01	9.32E-01	8.39E-01	5.27E-01
160	9.43E-01	9.15E-01	8.79E-01	9.80E-01	8.03E-01
180	1.00E+00	1.00E+00	9.99E-01	1.00E+00	9.98E-01

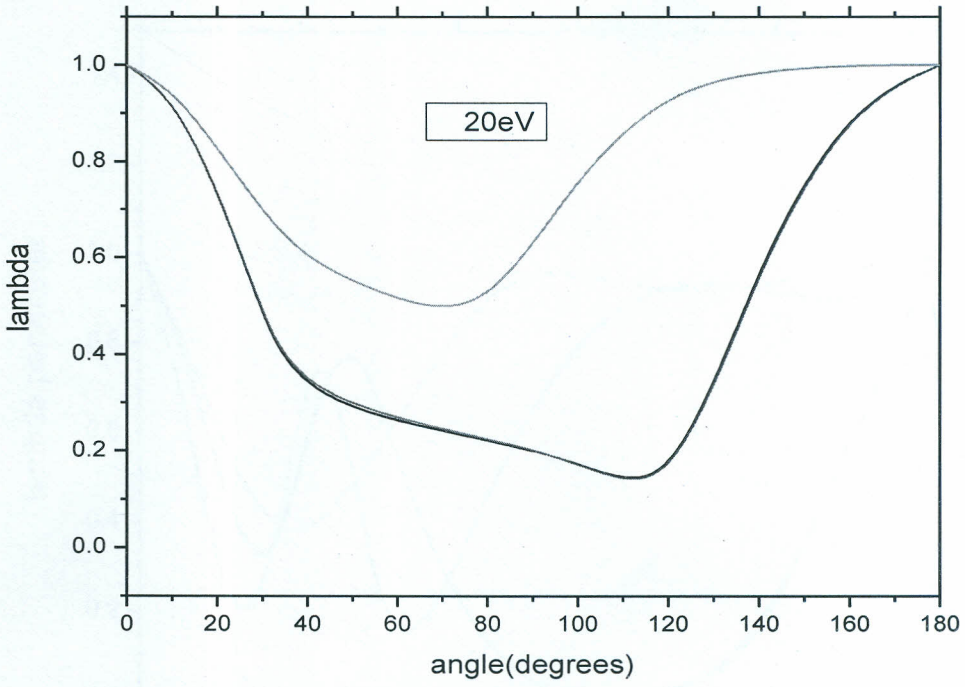

Figure 5.8 Present lambda parameter results for electron impact excitation of the lowest autoionizing state of rubidium at 20eV;

—— present static and exchange

—— present static,exchange and absorption

—— present static potential

—— Pangantiwar and Srivastava (1987)

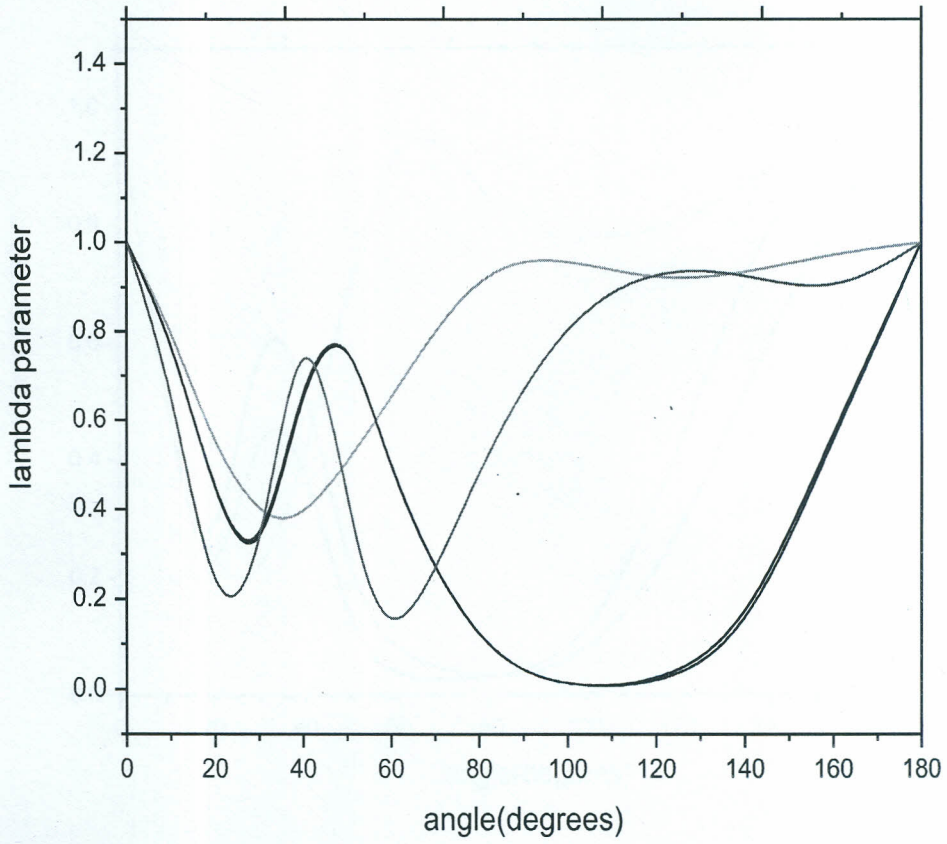

Figure 5.9. Present lambda parameter results for electron impact excitation of the lowest autoionizing state in rubidium at 30 eV;

—— Pangantiwar and Srivastava (1987)

—— present static potential

—— present present static and exchange

—— present static,exchange and absorption

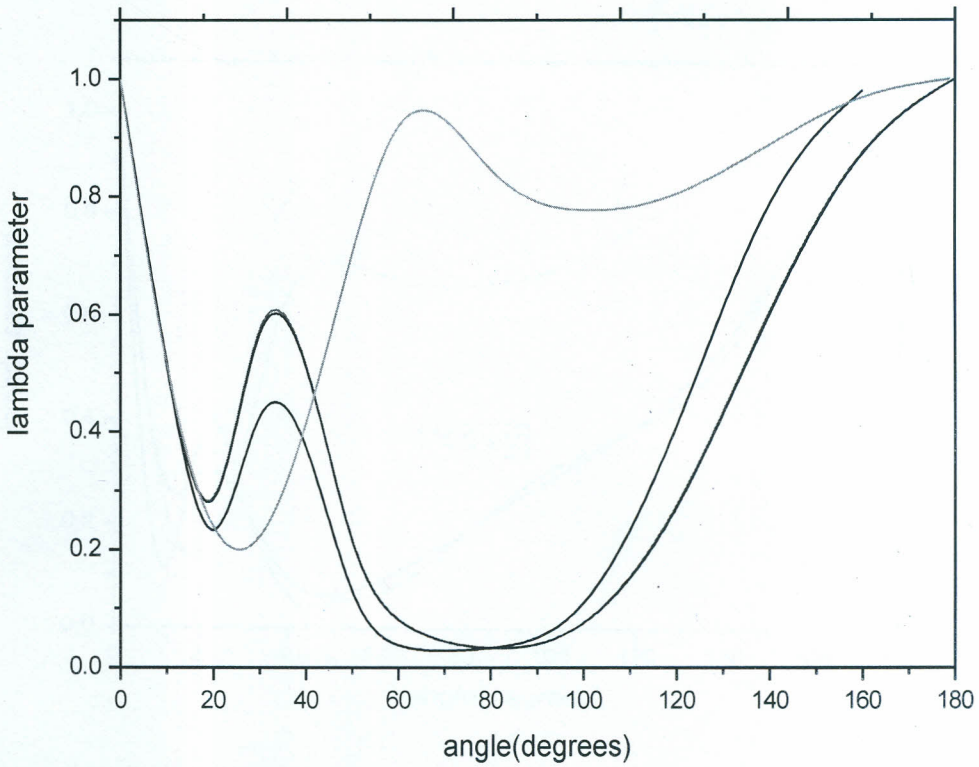

Figure 5.10.Present lambda parameter results for electron impact excitation of the lowest autoionizing state in rubidium at 50 eV;

—— present static and exchange

—— present static ,exchange and absorption

—— present static

—— Pangantiwar and Srivastava (1987)

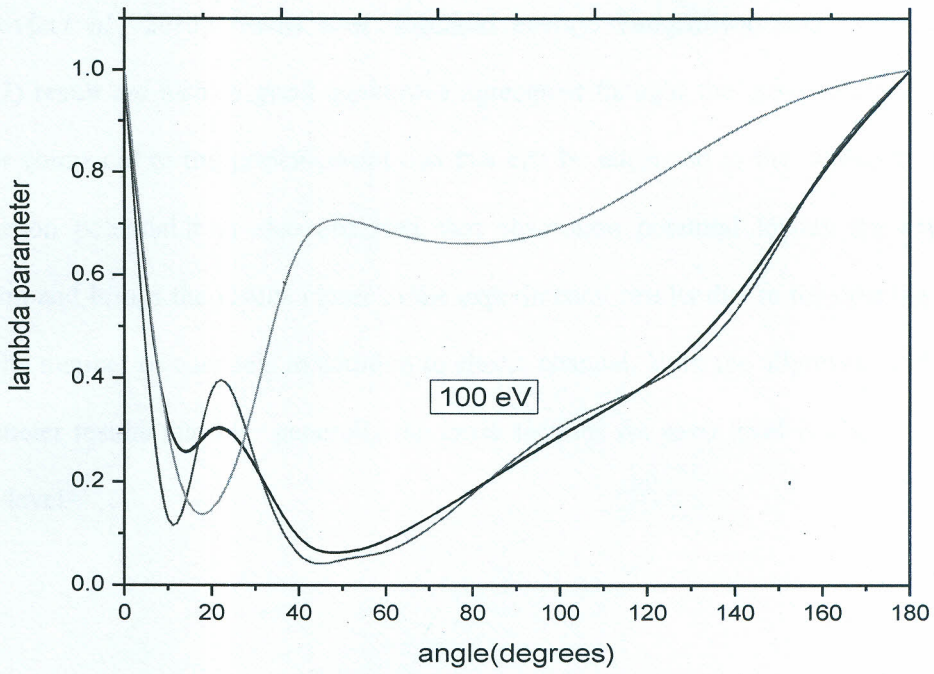

Figure 5.11.. Present lambda parameter results for electron impact excitation of the lowest autoionizing state in rubidium at 100 eV;

——— present static and exchange

——— present static,exchange and absorption

——— present static potential

——— Pangantiwar and Srivastava (1987)

5.5 Summary on results and discussions

The integral cross section results of this study (with absorption potential) for electron impact excitation of $4p^5 5s^2$autoionizing state of rubidium are in good qualitative agreement with the theoretical work of (Borovik *et al.*, 2012) and experimental (Borovik*et al.*, 2013) results near threshold energy. Pangantiwar and Srivastava (1987) result are also in good qualitative agreement thought the cross sections are lower compared to the present result and this can be attributed to the choice of the distortion potential.It is also observed that absorption potential lowers the cross section and brings the results closer to the experimental results due to the opening of infinite number of channels in addition to elastic channel. With the alignment and λ parameter results that the generally the cross sections for m=0 level is higher than m=1 level.

CHAPTER 6

CONCLUSIONS AND RECOMMENDATIONS

6.1 Conclusions

From this study, the following conclusions have been arrived at:

- The presentresults are in good quantitative agreement amongst themselves; compared toPangantiwar and Srivastava (1987) at all the projectile energies the present cross sections are relatively higher. This may the attributed to the choice of distortion potential which is more apparent at low impact energies than at high energies.The energy of the projectile determines the level of interaction in the target atom. Lower the projectile energy higher is interaction since the projectile spends more time in the vicinity of the target.
- Absorption distortion potential lowers the cross section at low energies and its and this is due to the opening of more channels at this point and considerable amount of time spent by the incident electron in the vicinity of the atom.
- Near threshold strong negative ion resonances (due to the existence of an extraelectron in the vicinity of the target atom electron cloud which makes the target behavelike a negative ion) there is sharp rise in the cross section though theexchange has less effect (Kaur and Srivastava, 1999).
- The lambda parameter indicates that more particles are scattered towards the magnetic sublevel m=0 for electron impact excitation atenergies close to excitation threshold.

- The alignment parameter results indicates that integral cross sections for m=0 are larger compared to m=1 up to about 400eV beyond which $\sigma 1 > \sigma 0$

6.2 Recommendations

The following recommendations may be considered for the purpose of improving results

obtained from this study:

- There is need for theoretical calculations on integral cross sections, differential cross sections, alignment parameter and lambda parameter for electron impact excitation of the lowest autoionizing state of rubidium using other quantum mechanical approaches such as the R matrix and convergent close coupling methods for comparisons.

- There is need for experimental work on the measurement of cross sections and angular correlation parameters for comparison purposes with the present results.

- There is need to include polarizationpotentialin the target's distortion potential in order to check its effect on the cross sections.

- There is need to include the second term of the distorted wave series DWBA2 to the firstterm DWBA1 in order to improve results of the distorted wave approximation for theproblem of electron impact excitation of the lowest autoionizing state of rubidium.

REFERENCES

Borovik,A.,Roman,V.andKupliauskien,A.(2012). The $4p^6$ autoionization cross section of Rb atoms excited by low energy electron impact. *Journal of Physics B: Atomic, Molecular and Optical Physics* **45:**1-6.

Borovik, A., Roman, V., Zatsarinny O. andBartschat, K.(2013). Electron impact excitation of the lowest doublet and quartet core-excited autoionizing states in Rb atoms. *Journal of Physics B: Atomic, Molecular and Optical Physics*. **46:**01520.

Bray, I.,Fursa, D.V.,Kadyrov,A.S.,Stelbovics,A.T.(2009) *The convergent close-coupling method for electron-atom scattering.*(Curtin University of Technology, Perth,Western Australia).

Burke, P.G. and Berrington, K.A. (1993). In *Atomic and Molecular Processes: An R-Matrix Approach.* (IoP, Bristol) pp 3 – 15.

Burke, P.G. and Berrington, K.A. (1993). In *Atomic and Molecular Processes: An R-Matrix Approach.* (IoP, Bristol) pp 3 – 15.

Clementi, E. and Roetti, C. (1974). Roothan–Hatree-Fock Atomic Wave functions.*Atomic Data and Nuclear Data Tables* **14**:177-478.

Feuerstein, B., Grum-Grzhimailo, A. N. and Mehlhorn, W.(1998).*Journal of Physics B: Atomic Molecular and Optical Physics.* **31:**593.

Furness,J.B. and McCarthy,I. E. (1973). Semiphenomenological optical model for electron scattering on atoms.*Journal of Physics B: Atomic Molecular and Optical Physics***6:** 2280.

Fursa, V. D. and Bray, I. (1995). Calculation of electron-helium scattering.*Physical Review A***52**:1279-1297.

Geltman,S. (1971) .Coulomb-projected Bornmethod.*Journal of Physics B: Atomic and Molecular Physic* **4**: 1288-1295.

Jabloski, A., Salvat, F. and Powell, C.J. (2004). Comparison of Electron-Elastic-Scattering Cross Sections Calculated from Two Commonly used Atomic Potentials. *Journals of Physics.*Chem.33, 409- 451.

Joachain, C. J. (1975). *Quantum Collision Theory.*North Holland Publishing Company, Amsterdam.

Jobunga, O. (2009). Electron impact of the lowest autoionizing states of alkalis using a distorted wave method. M.Sc. Thesis, Kenyatta University.

Katiyar,A.K.,Srivastava,R. and Rai,D.K.(1989).Distorted wave approximation for e-He (1^1S-2^1P) excitation: Angular correlation and differential cross-sections.*Physical Review A***40**:27492752.

Kaur.S. and Srivastava, R. (1999). Excitation of the lowest autoionizing$np^5(n+1)s^2$, $^2P_{3/2,1/2}$ states of Na(n = 2), K(n = 3), Rb(n = 4) and Cs(n = 5) by electron impact.*Journals of Physics B: Atomic, Molecular and Optical Physics* **32**: 2323.

Madison, D. H. and Bartschat, K. (1996). The distorted wave method for elastic scattering and atomic excitation.*Computational atomic physics.* Springer Verlag, Berlin.pg 46.

Matterstock B, Huster R, Paripas B, Grum-GrzhimailoA N and Mehlhorn, W. (1995).

Excitation of K*(3p54s2 *2P3p,* 2P1/2) by electron impact in the range from near threshold to

500 eV: alignment and cross section ratios.*Journals of Physics B: Atomic, Molecular and*

*Optical Physics.***28**: 4301.

Mayaka, Job Oqhoyho (2010). Electron impact double excitation of (2s2) ^1S and (2s2p) ^1P states of helium atom using a distorted wave method.*M.Sc.Thesis, Kenyatta University.*

McCarthy, I.E. and Weigold, E. (1995). In Electron-Atom Collisions. (Cambridge University Press, Cambridge). pp 156 – 190.

Mcconkey .J.W. (2005).*Electron collision-past, present future.NP4*(WindsorOntario,Canada).

Nygaard, J., (1975). Electron impact autoionization in heavy alkali metals. *Physical review A***11**: 4.

Oketch, F. O. (2013). Distorted wave method applied to electron impact excitation of the lowest autoionizing state of rubidium.*M.Sc.Thesis, Kenyatta university.*kenya.

Pangantiwar,A. and Srivastava,R. (1988). Excitation of the rubidium atom by electrons and positrons: differential cross section and correlation parameters. *Journals of Physics B: Atomic Molecular and Optical Physics***21**:4007-4013.

Pangantiwar, A. W. andSrivastava, R. (1987).$e^{\pm}$impact excitation of autoionizing levels in alkalis: a distorted-wave approach. *Journal of Physics B:Atomic and Molecular Physics* **20**:5881-5902.

Ross,K.J. and Ottely, T.W.(1975). Ejected electron spectrum of rubidium autoionizing levels obtained by electron impact excitation. *Physical Letters A***54**: 57-58.

Roy, B. N. and Rai, D. K. (1973). Electron-impact ionization of alkali metals.*Physical Review* A 8: 849-855.

Saxena, S. and Srivastava, R. (2004). Electron impact excitation of rubidium atoms.*The European Physical Journal department* **30**:23-35.

Schaub-Shaver, J. A. and Stauffer, A. D.(1980). The variable-charge Coulomb-projected

Born approximation. *Journal of Physics B: Atomic and Molecular Physic* **13**:7.

Scott, M. P. (2004).*Introduction to R-matrix theory in atomic Physics.*EU Socrates

Intensive Programme.

Singh,C.S.(2004). Magnetic-sublevel differential cross sections for electron impact of 2^1P state of helium.*East African Journal of Physical Sciences* **5**:85-98.

Singh, C.S. (2013). Effect of exchange and absorption potential in the distorted wave calculation of electron impact excitation of autoionizing state of lithium.*Abstract of contributed papers.XXVIII ICPEC, (Lanzhou, China).*

Srivastava, R. and Singh ,C.S. and Rai, D.K. (1982). Excitation of the lowest autoionizing states in alkalis. *Journal of physics B: Atomic and Molecular and Optical Physics* **15**: 1899-1903.

Stapelfeldt, H., Krisgtensen, P., Ljungblab, U. and Anderson, T. (1994). Autoionizing states of negative ions in strong resonant laser fields: the negative rubidium ion. *Physical Review A50:*1618.

Staszewska, G., Schwenke, W.D. and Truhlar, G. D (1984). Non-empirical model for the imaginary part of the opticalpotential for electron scattering.*Journal of physics B: Atomic and Molecular and Optical Physics*. **16**:L281-L287.

Stauffer, A.D. and Morgan, L.A (1975).A generalization of the Coulomb-projected Born

approximation.*Journal of Physics B: Atomic and Molecular Physic* **8**:13.

TheodosiouConstantine, E. (1987). Collisional excitation and alignment of np^5 (n + 1) s^2autoionizing states of the alkali-metal atoms.*Physics Review A* **36**:3139-3145.

Tiwary, S.N. and Rai, D.K.(1975). Electron impact excitation of the lowest autoionizing level in alkali atoms.*Journal of Physics B: Atomic and Molecular Physics* **8**:1109-1113.